ARL 64-49
MARCH 1964

Aerospace Research Laboratories

BASIC RESEARCH ON GAS FLOWS THROUGH ELECTRIC ARCS-HOT GAS CONTAINMENT LIMITS

G. L. CANN
R. D. BUHLER
R. L. HARDER
R. A. MOORE
ELECTRO-OPTICAL SYSTEMS, INC.
PASADENA, CALIFORNIA

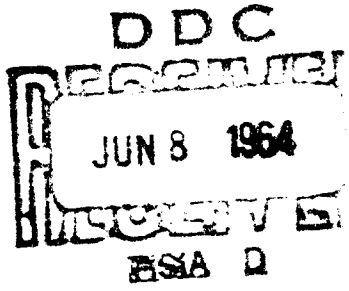

OFFICE OF AEROSPACE RESEARCH

United States Air Force

NOTICES

When Government drawings, specifications, or other data are used for any purpose other than in connection with a definitely related Government procurement operation, the United States Government thereby incurs no responsibility nor any obligation whatsoever; and the fact that the Government may have formulated, furnished, or in any way supplied the said drawings, specifications, or other data, is not to be regarded by implication or otherwise as in any manner licensing the holder or any other person or corporation, or conveying any rights or permission to manufacture, use, or sell any patented invention that may in any way be related thereto.

- - - - - - - - -

Qualified requesters may obtain copies of this report from the Defense Documentation Center, (DDC), Cameron Station, Alexandria, Virginia.

- - - - - - - - -

This report has been released to the Office of Technical Services, U. S. Department of Commerce, Washington 25, D. C. for sale to the general public.

- - - - - - - - -

Copies of ARL Technical Documentary Reports should not be returned to Aerospace Research Laboratories unless return is required by security considerations, contractual obligations or notices on a specified document.

500 - May 1964 - 162-39-774

ARL 64-49

BASIC RESEARCH ON GAS FLOWS THROUGH ELECTRIC ARCS-HOT GAS CONTAINMENT LIMITS

G. L. CANN
R. D. BUHLER
R. L. HARDER
R. A. MOORE

ELECTRO-OPTICAL SYSTEMS, INC.
PASADENA, CALIFORNIA

MARCH 1964

Contract AF 33(657)-7940
Project 7063
Task 7063-03

AEROSPACE RESEARCH LABORATORIES
OFFICE OF AEROSPACE RESEARCH
UNITED STATES AIR FORCE
WRIGHT-PATTERSON AIR FORCE BASE, OHIO

FOREWORD

This interim technical report was prepared by Electro-Optical Systems, Inc., Pasadena, California, on Contract AF 33(657)-7940 for the Aerospace Research Laboratories, Office of Aerospace Research, United States Air Force. The research reported herein was accomplished on Task 7063-03, "Energy Exchange Phenomena in Electric Arc Discharges" of Project 7063, "Mechanics of Flight" under the technical cognizance of Mr. Charles A. Davies of the Thermo-Mechanics Research Laboratory of ARL. This research is part of a larger program on electric arc discharges which is being conducted by the Thermo-Mechanics Research Laboratory.

The report includes some data obtained from Contract AF 33(657)-8839 of the Air Force Aero Propulsion Laboratory, Research and Technology Division, Air Force Systems Command. Permission of the contract monitor, Mr. F. J. L'Hommedieu, Jr., to include that information is gratefully acknowledged.

ABSTRACT

Extensive measurements in a "cascade" type arc research apparatus were carried out with four gases (hydrogen, helium, ammonia, and argon), covering both the inlet region and the fully developed region of the coaxial flow discharge. The inlet (gas heater) region results for three gases were compared with the Stine-Watson first order theory. For the size-pressure regime in which radiation can be neglected, the Stine-Watson relations with empirically adjusted constants gave a satisfactory semi-empirical description of all the inlet cases investigated.

To estimate the ultimate technical limits of arc gas heater performance the well known approximate theories for the fully developed arc column (Parabola and Bessel Models) were extended to include radiation and, (for the high current regime) the self-magnetic pressure gradient. Hot gas containment limits (highest radially-averaged outlet enthalpy vs. pressure) were calculated for air, for a range of allowable wall heat loads (0.1-10 kw/cm^2). This resulted in a predicted "absolute" technical limit of continuous hot gas containment independent of size, within the pressure-size range of the optically thin gas approximation.

The theoretical containment limit curves appropriate for a highly cooled thin metal wall (say 3-10 kw/cm^2) fall substantially above the (previously published) empirical "state of the art" performance envelope for continuous operation. Thus, it is concluded that:

(1) Heat loads from mechanisms other than the simple hot gas containment (e.g. electrode heat loads, local secondary arcs, etc.) have so far limited the enthalpy-pressure values achieved.

(2) Gas heater performance substantially above the 1961 state of the art curve appears technically possible, with optimum designs.

TABLE OF CONTENTS

LIST OF FIGURES

LIST OF SYMBOLS

E	Electric Field
h	Enthalpy
I	Total Arc Current
j	Current Density
K	Thermal Conductivity
$\dot{m}$	Mass Flow Rate
P_r	Radiated Power per Unit Volume
P_s	Power Transferred to an Individual Column Segment
q	Heat Flux
Q	Cumulative Power into the Arc Column Segments
r	Radius
R	Radius of Column
V	Voltage along Arc Column Measured from Entrance (here from the cathode)
w	Axial Gas Velocity
z	Axial Distance Along Arc Column
ϕ	Thermal Conductivity Integral or Heat Flow Potential
ρ	Gas Density
σ	Electrical Conductivity

Subscripts

w	Wall Value
∞	Asymptotic Value

1. INTRODUCTION AND SUMMARY

The technology of the arc gas heater or plasma source is relatively new, in spite of the vast background of arc technology. Electric arcs have been studied for nearly a century, and utilized very extensively for many applications since the turn of the century. However, except for a few chemical processing applications, the primary purpose of most arcs was either the melting of solid substances or the production of visible and UV radiation, rather than the production of arc plasma for its own sake. Still other important applications are those in which the arcs are unwanted and destructive and must be "quenched" or blown out (e.g., switch gear).

In the past 10 or 15 years a number of new technical fields have arisen which specifically require very hot gas (or plasma) above the chemical combustion temperature regime and at relatively high densities, pressures and velocities. Among these fields are, starting from the low temperature end:

The spraying and welding of refractory materials
The simulation of atmospheric re-entry flight conditions, i.e. plasma wind tunnels and heat shield test jets
Electric (plasma) rockets for space propulsion
Some aspects of thermonuclear fusion and astrophysics research.

For several of these applications the plasma generator must operate continuously at the highest technically possible gas temperatures or enthalpies, and at pressures ranging from about one to several hundred atmospheres.

The arc gas heater (or arc jet) is to date the most practical and versatile continuous source of high density plasma, though it can and will be augmented by various methods of magnetogasdynamic ("MGD") pumping. As a result the design of arc devices for the heating of gases has been developed as a highly specialized art over the past decade. Many configurations for the interaction of the arc and the gas flow have been

evolved, mostly empirically and intuitively, and used with varying degrees of success in the construction of wind tunnel gas heaters and laboratory models of plasma rockets.

It is the purpose of this report to contribute to the understanding of the arc jet gas heater performance and its limitations. It is hoped that the results presented will:

Lead to more reliable long range estimates of the ultimate performance potentials* (in terms of pressure-enthalpy envelopes) of such devices, for different gases, sizes and other conditions

Permit much more efficient and less costly development of specific devices than was possible by purely empirical methods, and where necessary, a closer approach to the "ultimate" technical limits of performance.

All the results presented in this report apply to one particular arc gas heater configuration which we call the "coaxial flow discharge". In this the arc discharge and the gas to be heated are passed through a cylindrical discharge tube or "constrictor" (Fig. 1). This general arc gas heater geometry or family based on the use of such a constricted flow discharge has been found to yield the highest mean gas temperatures (or enthalpies) among the many geometries which have been studied and tried; and there are good physical reasons why this is so.

However, some of the analytical results presented here are perhaps of more general validity than the performance limits of a specific geometry or configuration would suggest. The "hot gas containment limits", though calculated for the specific coaxial flow discharge case, are likely to be at least approximately applicable to any hot gas contained in or flowing continuously through a solid walled container or nozzle throat, regardless of the method by which the gas was heated. The reason is that, as long as heat conduction to the "cool" walls is a major factor** the temperature profiles across such a hot gas flow will quickly approach some "near parabolic" shape. For the radiation contribution to the wall heat load, the detailed temperature and pressure distributions are relatively unimportant, within the "thin gas" approximation used here. Thus, the relations between mean enthalpy, mean

* Barring some breakthrough advance in materials or in gas heater concepts

** We are speaking here of average gas temperatures between ~20,000 and 30,000°K or higher, while a solid wall of any known material will be below ~4200°K

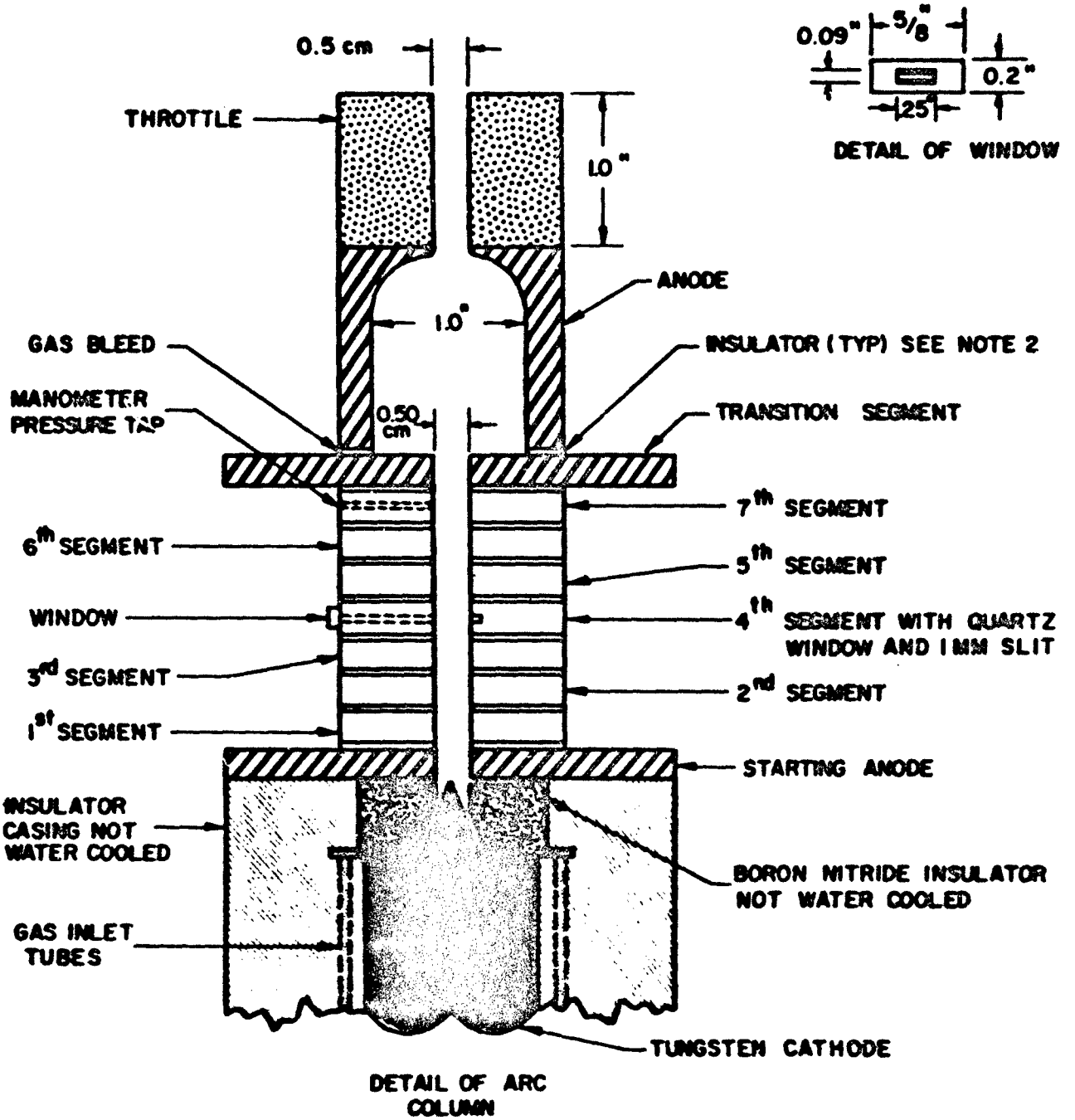

DETAIL OF ARC COLUMN

NOTE:

1. ALL COMPONENTS WATER COOLED UNLESS OTHERWISE NOTED
2. ALL INSULATORS BETWEEN COMPONENTS ARE A COMPOSITE OF BORON NITRIDE, TRANSITE & SILICON RUBBER

FIG. 1 ARC COLUMN SCHEMATIC

pressure and wall heat loads which are given, should be approximately valid for any general case within the regimes treated.

The flow discharge through a cylindrical tube may be roughly subdivided into two regimes, if the discharge tube is sufficiently long. From the end where the cold gas flows in (with the arc column in the center) to some distance downstream we have the "inlet" or "gas heater" region in which the mean enthalpy of the gas and the properties of the discharge change rapidly in the axial direction until all the discharge and gas parameters (except the pressure) approach some asymptotic condition (to within a specified accuracy). From that point on, the arc and the gas flow and temperature distributions remain substantially unchanged except for the slight axial pressure gradient and a corresponding small positive axial velocity gradient. This is designated as the "asymptotic" or "fully developed" constricted arc column region or "arc heated Poiseuille flow".*

The inlet or gas heater region is the most important one for engineering applications, i.e., for arc jet gas heaters. However, the asymptotic regime, which is mathematically as well as experimentally much simpler, gives considerable insight also into the performance limits of the heater regime. The asymptotic "infinitely long" constricted arc column (with or without laminar coaxial gas flow) has been extensively studied at least since the early 1930's, and there is a vast body of literature on this "classical" problem. Most of this is well summarized in Refs. 3,4 and 2. The inlet region and other flow discharge cases with axial gradients have been worked on intensively only in the last few years, except for an outstanding series of experimental studies on switch blow-out published at the Siemens Laboratories in the 1930's (Ref. 6). Only very few papers deal with such discharges analytically. (Refs. 6, 7, 8, 9, 10)

The present report utilizes and extends results for both the Asymptotic or Fully Developed Arc Column and the Inlet Region. The first part of the report deals with cases (pressure, tube size, gas type) for which the radiation from the gas to the wall is unimportant compared with thermal conduction. The first order analysis of the inlet region by Stine and Watson (Ref. 8) but with empirically adjusted material function constants

*These flow regimes and the approximate methods used to describe and analyze them are discussed in Refs. 1, 2, 5, and 23.

(i.e., using "effective" transport coefficient derivatives) is compared with experimental measurements in three different gases, each over a range of current and mass flow values. This shows that the Stine-Watson theory, in spite of its drastic simplifications, leads to a satisfactory engineering description of the inlet region where radiation is negligible.

From the empirically adjusted Stine-Watson relations one now has a relation between the radially-averaged enthalpy of the gas at the heater outlet and the wall heat load, for the case of pure conduction only. This gives the first approximation to the "hot gas containment limit" on the enthalpy pressure chart for small arc heaters of specified size, but it cannot give an "absolute" containment limit. According to this description, the "attainable" enthalpy would increase indefinitely with increasing size. More precisely stated: this theoretical model, which neglects radiation, loses even qualitative validity above certain size-pressure (or power) levels where the radiative heat transfer becomes dominant.

To obtain a valid "absolute" limit for the containment of the hot gas in a cylindrical constrictor, the radiation contribution to the wall heat load must be included. Before discussing this we point out that, for the calculation of this performance limit, i.e., for the relations between wall heat load and mean gas enthalpy and pressure, we do not need an inlet flow theory, since the inlet (or gas heater) flow discharge approaches asymptotically the fully developed tube stabilized column case. If one attempts to achieve high mean gas enthalpies in an arc heater, the constrictor must be long enough so that the fully developed end condition is closely approached (say to within 10 percent). Thus the wall heat loads near the heater outlet will also closely approach the heat loads of the fully developed flow-column. Thus the theory of the fully developed flow-column, i.e., the asymptotic limit of the heating process, is sufficient for these order of magnitude calculations of the containment limit. For this we use the "Bessel model" of the arc column together with the linearized calculation of the mean enthalpy as used by Stine and Watson.

In line with the approximate nature of this calculation, various simple approximations to the radiation from the gas are introduced into the column theory. One of these (designated as Law No. 3 on Fig. 14) is valid for moderate temperatures (up to ~15,000°K, for the gases of interest here). This represents the logical extension of the Bessel model to include radiation. The accuracy of this approximation is verified by experimental measurements covering this temperature range. On the performance limit chart, this lower temperature regime covers the highest pressures.

With radiation included the containment limit calculation immediately leads to an optimum constrictor or tube size, which lies where the radiative and conductive heat load contributions are about equal. This also specifies an approximate optimum power level for the heater at each pressure-enthalpy point. These are probably the most important qualitative results of the study. When the optimum size and the allowable wall heat load are chosen the calculation then gives an "absolute technical limit" line on the pressure-enthalpy plane for continuous gas heaters, over the regions where the various approximations are valid.

The validity of the "optically thin gas" approximation, used throughout this study, is verified a posteriori for each case. That is, the calculated containment limit is considered valid as long as the optimum size and pressure value obtained lies within the thin gas region by several orders of magnitude.**

Another simple approximation to the radiation and electric conductivity functions (designated as Law No. 1 on Fig. 12) appears suitable for the ~15,000-30,000°K range in nitrogen, argon and similar gases, i.e., for the highest attainable enthalpies at low pressures. This results in the well known Wire or Parabola model of the arc column with radiation (Ref. 4). In calculating the limiting enthalpies it was found that

---

** The containment limit based on the thin gas assumption represents a "local" maximum. Hence we must consider the possibility of exceeding this limit with an extremely large device where self absorption would predominate. The check assures us that this size, if it exists, is beyond the realm of present practical consideration.

the total current values became high enough that the magnetic "pinch" pressures would be an appreciable fraction of the gas pressure in the center of the arc. Hence this pressure correction was included. This containment calculation for the wall stabilized discharge must be terminated when current and pressure values are reached which make the wall pressure go to zero, i.e. where the magnetic containment begins.

The new containment limit curves on the enthalpy-pressure plane are compared with a purely empirical enthalpy pressure envelope of wind tunnel arc gas heaters, compiled recently (Ref. 11). They show surprising similarity in the high pressure region where the current values are moderate (a few hundred to a few thousand ampere). In the low pressure regime, the enthalpy limits of the containment calculation are much higher than those achieved in practice, but the corresponding total current values also are extremely high (~ 10,000 - 70,000 amp). Hence in this regime the gas heater performance appears limited not by the simple hot gas containment calculated here, but by other technical limits, presumably on the electrodes.

2. [illegible]

2.1 Description of Apparatus

For the experimental study of the interaction between the positive column region of an electric arc with gas flowing coaxially with the arc, an apparatus was fabricated consisting principally of an arc-column containment section, a cathode, and an anode assembly. The assembled apparatus is shown schematically in Fig. 1 and in the photograph of Fig. 2. The main functions of this apparatus are to provide for:

Extending the positive column of the arc over a sufficiently long distance through a circular cylindrical channel that influences of the electrode attachment regions on the gas-column interaction are negligible.

Measuring the gradient of: (a) energy transfer from the column to the walls of the channel, (b) electric potential, (c) gas pressure.

The apparatus was mounted vertically to a tubular test chamber equipped with a pyrex port for viewing the effluent from the arc apparatus and a cooler for cooling the gas. The test chamber was in turn connected to a vacuum pump.

The column containment section is made up of water-cooled copper segments, each of which is electrically and thermally insulated from adjacent segments or components of the apparatus. These segments have an internal diameter of .5 cm and are .25, .50 or 1.0 cm thick. The assembled column section was varied in length from 5 to 10 cm. Insulators for the segments consist of an inner disk of boron nitride surrounded by an outer disk of transite. The outer edge of the transite is coated with a thin film of silicone rubber to form a gas seal. The boron nitride disk fits inside the transite disk with contact at three small tabs equally spaced around the periphery of the boron nitride disk. These tabs maintain the disks concentric with the holes in the column segments while limiting the heat conduction to the outer disk. The thickness of the insulators is about 1.0 mm.

Each segment forming the column containment section of the apparatus is separately cooled by water which flows through a circular finned passage.

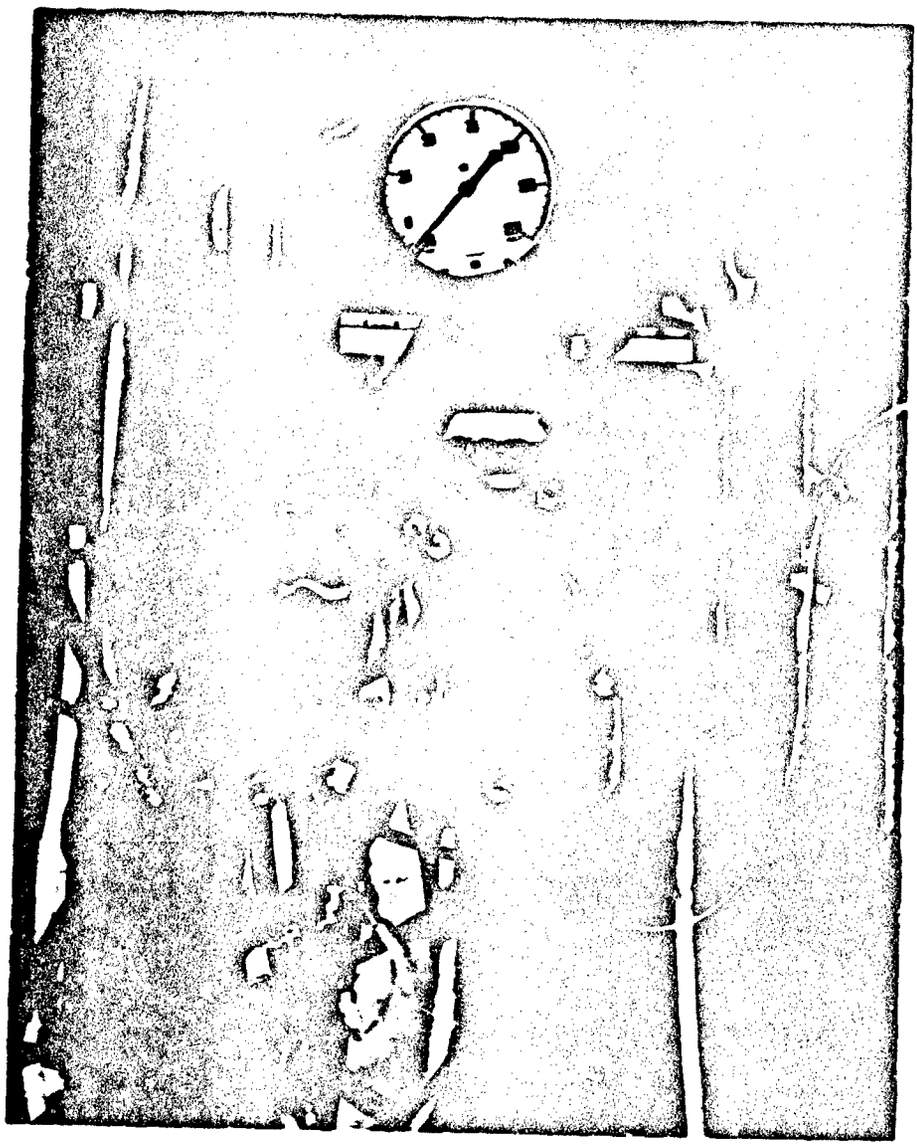

FIG. 2 ARC COLUMN APPARATUS

Heat flux values above 10 kw/cm^2, based on the internal cylindrical surface area, have been measured with these segments.

A conical tungsten cathode was used for these experiments. The point of the cathode was located at the inlet of the first segment.

It is common practice in arc heaters to introduce the gas into the heating chamber by tangential injection causing the gas to flow through the heating region with a vortex motion. Considerable speculation as to the usefulness or desirability of this vortex has occurred and no concrete answers have yet emerged. For this reason, the experiments were carried out with gas injected both axially and tangentially near the cathode tip. In the latter case the angle of injection was held constant at 20°.

The anode assembly is located adjacent to the gas exit end of the column section. After starting the arc to the first segment, power supplies connected between the cathode and the anode assembly are energized and the arc through the column containment section is established. The anode is of a diameter several times larger than the column section to provide for the capability of very large currents before exceeding cooling heat flux limits at the anode. The arc attachment point of the anode surface is caused to rotate around the anode by a solenoid coil which surrounds the anode. The magnetic field produced by this coil is limited to a negligible strength outside of the anode region by an iron housing around the coil.

A second gas inlet is provided in the anode. It is possible to bleed argon in through this hole, so that the anode attachment point will always occur in an atmosphere of argon, independent of the type of gas flowing through the column. Experience has indicated that anodes suffer least erosion and behave most stably, when the ambient gas is argon. This auxiliary gas inlet also provides a means of controlling the gas pressure. Since all of the gas passes through a sonic orifice between the anode and the vacuum pump, the pressure in the column can be controlled by changing the mass flow of gas through the second gas inlet. It was possible to control the pressure to within $\pm$ 3 mm at pressure levels of over one atmosphere using this technique.

2.2 Measurements

The variables measured during these experiments are as follows:

a. arc current

b. voltage of each segment

c. total arc voltage

d. heat transfer rate to each segment

e. static pressure at each segment

f. gas mass-flow-rate.

Also, in more recent experiments, some of the segments were equipped with quartz viewing ports; measurements were made of radiation intensity and temperature distribution by spectroscopic methods.

Some difficulty was encountered in making accurate measurements of the potential distribution in the column. One reason for this is that the ionized gas is surrounded by an annulus of cold un-ionized gas, especially near the inlet. This then makes it somewhat uncertain as to what potential the segment will assume relative to the potential of the gas on the axis at that position. Without any real justification, it was assumed that the measured segment potential reflected the average potential in the gas over that segment. Some rather elaborate calculations on radial potential distribution and sheath potential drops would have to be made in order to obtain more accurate estimates of the relation between the measured potential and the true electric potential on the axis of the discharge.

The current range covered in the experiments was from 100 to 200 amperes. The mass flow rate was varied from .070 gm/sec to .250 gm/sec.

2.3 Results

From the experimental data the following heating rate and heat loss rate parameters were calculated:

Heating Rate Parameter: $\frac{2\pi V}{\dot{m}}$

Heat-Loss Rate Parameters: $\frac{2\pi Q}{\dot{m}I}$

From the Stine-Watson approximate solution (Ref. 8) for the arc column with a coaxial gas flow, these parameters are seen to depend essentially

only on a dimensionless arc length given by:

$$z/z_o = z/\dot{m}\left(\frac{dh}{d\phi}\right) \sim z/\dot{m}$$

Typical results, those with helium, are shown in Figs. 3, 4 and 5 where $\frac{2\pi V}{\dot{m}}$ and $\frac{2\pi Q}{\dot{m}I}$ are plotted against the length parameter, $z/\dot{m}$.

The data in Fig. 4 for tangential injection of the gas are virtually identical to the data in Fig. 3 taken when the gas had no vorticity. On the other hand, the results shown in Fig. 5 from a seperate experiment also with tangential injection, indicate significant differences from the other data. Much more power is transferred to the inlet segments and the difference between the two curves of $2\pi V/\dot{m}$ and $2\pi Q/\dot{m}I$ remains much lower than was observed in the other tests. Tentatively these differences are explained by assuming that the primary vortex became unstable resulting in secondary flows which carried hot gas from the arc region back onto the surfaces of the inlet segments. This would tend to increase the heat flux into the segments near the inlet while simultaneously reducing the average gas enthalpy. The implication from these results would appear to be that the vorticity in the gas does not make any marked improvement in the gas heating process while seriously degrading the heating capability of the arc if the vortex becomes unstable and sets up secondary flows.

Points were read off the average curves through the data of Fig. 3 in order to obtain the efficiency and fraction of maximum enthalpy as a function of the coordinate $z/\dot{m}$. The value found for the maximum enthalpy can be expressed as follows:

$$\frac{2\pi h_m}{I} = .239 \times 10^4 \frac{\text{meters joules}}{\text{Kgm. amp.}}$$

This quantity, as shown in Fig. 3, is just the difference between the two curves $2\pi V/\dot{m}$ and $2\pi Q/\dot{m}I$ in the region where these curves have become parallel to each other.

2.4 Correlation of the Experimental Data with the Stine-Watson Theory

There are several techniques available to use in an effort to obtain a correlation between the experimental data presented in Section

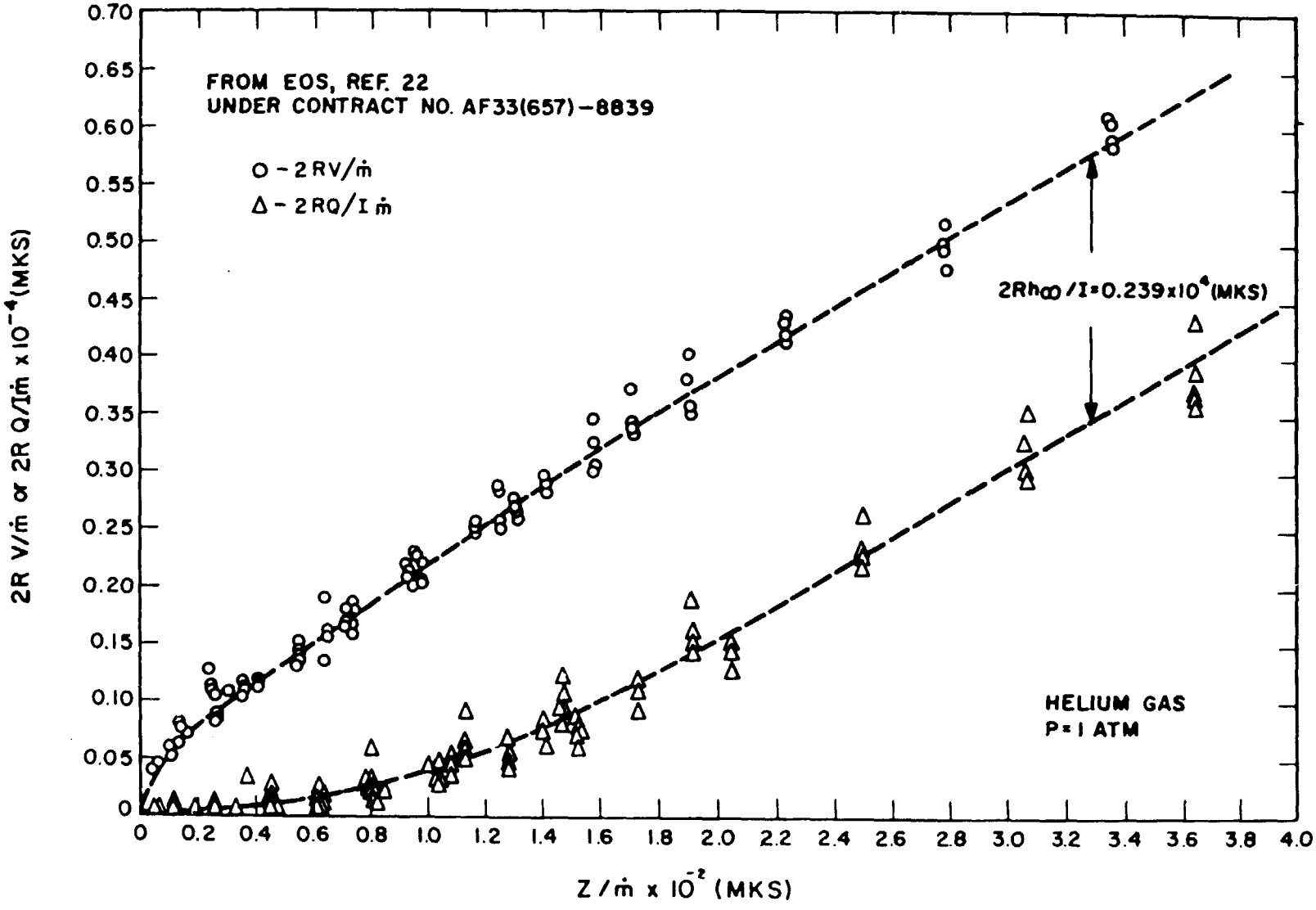

FIG. 3 SIMILARITY PLOT SHOWING GAS HEATING RATE FOR HELIUM FLOWING AXIALLY IN A SEGMENTED COLUMN

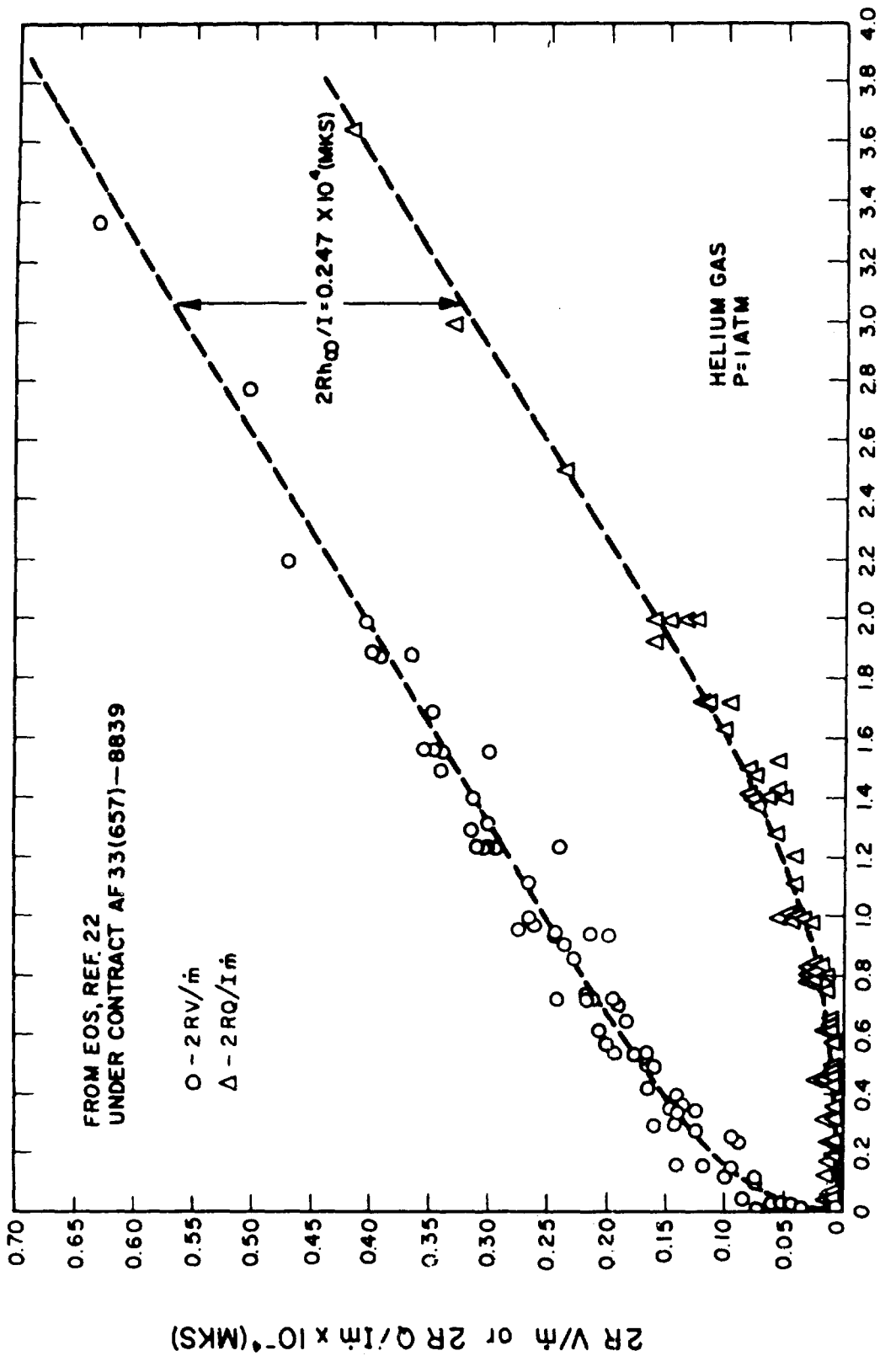

FIG. 4 SIMILARITY PLOT SHOWING GAS HEATING RATE FOR HELIUM WITH TANGENTIAL INJECTION FLOWING IN A SEGMENTED COLUMN (STABLE)

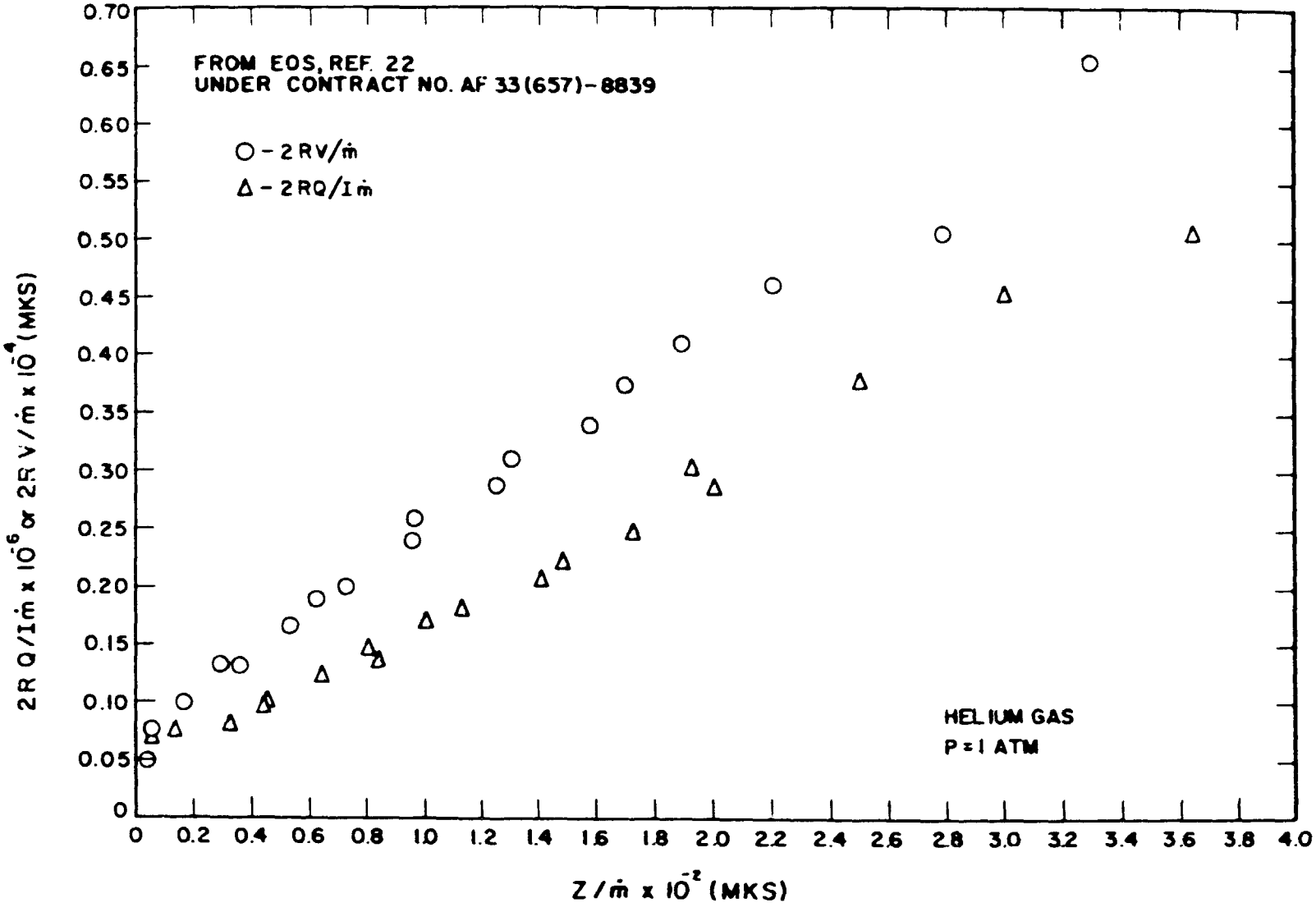

FIG. 5 SIMILARITY PLOT SHOWING GAS HEATING RATE FOR HELIUM WITH TANGENTIAL INJECTION FLOWING IN A SEGMENTED COLUMN (UNSTABLE)

2.3 and the theory of Stine and Watson. The most direct method would be to plot curves of enthalpy and electrical conductivity vs. the thermal conductivity integral and evaluate the slopes of a linear approximation to these curves. This would then enable us to evaluate the quantities

$$z_o = \frac{h}{\pi} \left(\frac{dh}{d\phi}\right)$$

and

$$E_\infty = \frac{2.4}{R} \left(\frac{d\phi}{d\sigma}\right)^{1/2}$$

Using these quantities, it would be possible to plot the experimental data on a universal non-dimensional plot of

$$\frac{V}{z_o E_\infty} \text{ vs. } \frac{z}{z_o}$$

and

$$\frac{Q}{2\pi R q_\infty z_o} \text{ or } \frac{\Sigma P_s}{z_o E_\infty I} \text{ vs. } \frac{z}{z_o}$$

These plots of experimental points could then be compared with the theoretical curves for these quantities that are presented in Ref. 8. This approach was not feasible at the time the data were reduced since the transport coefficient data necessary to obtain these curves were not available. An alternative approach, which works backward from the experimental data, is outlined below.

From the curves drawn through the experimental points (e.g., Fig. 3) it is possible to determine efficiency of energy transfer to the gas and the ratio of the local average gas enthalpy to the asymptotic gas enthalpy, which was evaluated in Sec. 2.3. Data representative of these quantities for helium, hydrogen and ammonia are shown in Fig. 6. The shapes of the efficiency curves for helium and hydrogen near the inlet indicate, by comparison with the theoretical curve of Stine and Watson that the measured efficiencies are significantly higher than the predicted efficiencies. The theoretical curves have only one curvature, whereas the experimental curves go through a reversal of curvature near the inlet. It was decided to extrapolate the efficiency curves for helium and hydrogen up to the value one

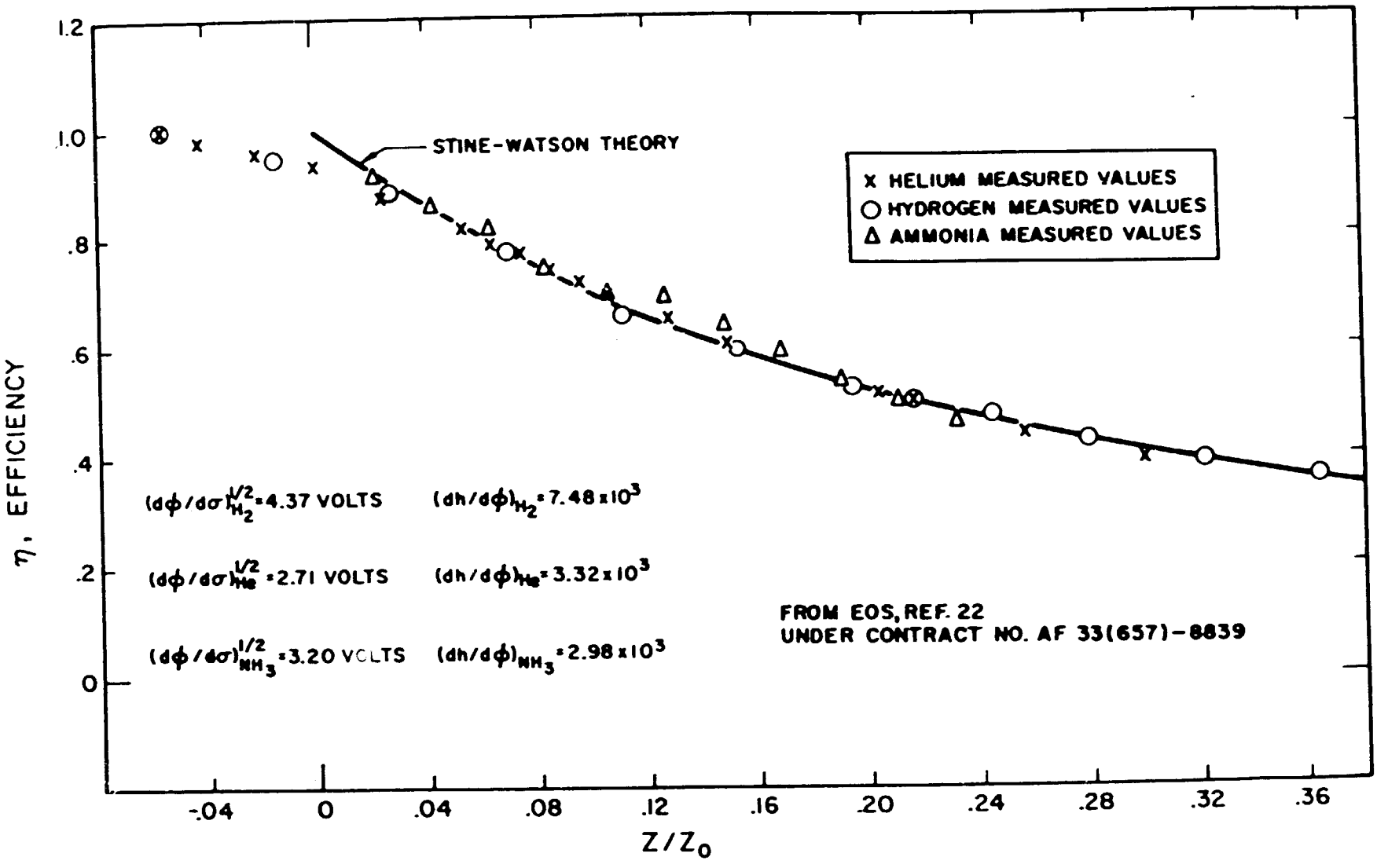

FIG. 6 COMPARISON OF EFFICIENCY IN THE ARC COLUMN WITH THEORETICAL VALUES

at the curvature exhibited over most of the curves.

The values of $z/\dot{m}$ where the efficiency curve intersects the value one was taken as a new origin. The value of $\frac{dh}{d\phi}$ was then computed from the value of $z/\dot{m}$ where the efficiency was equal to 0.50. The equation for evaluating the quantity is given below:

$$\left(\frac{dh}{d\phi}\right) = \frac{\pi}{.213}\left(\frac{z}{\dot{m}}\right)_{\eta = .5}$$

The quantity $\left(\frac{z}{\dot{m}}\right)_{\eta = .5}$ is the corrected value for the extrapolated efficiency curve as described above. In this way, the experimental and theoretical curves were fitted at efficiencies of 0.5. It was then possible to plot points from the experimental efficiency curves onto the theoretical efficiency curve over the whole range of z/z_o for comparison. This was done to obtain the results presented in Fig. 6. It is seen from this figure that, with the rather arbitrary shift in origin used, the agreement between the experimental points and the theoretical curve is satisfactory.

From the values of $\left(\frac{2Rh_\infty}{I_{P_s}}\right)$ determined from the asymptotic difference between curves of $V/\dot{m}$ and $\frac{\mathcal{E}}{\dot{m}\, I}$, it was possible to evaluate the quantity $\left(\frac{d\sigma}{d\phi}\right)^{1/2}$.

$$\left(\frac{d\phi}{d\sigma}\right)^{1/2} = \frac{1}{.266}\left(\frac{2Rh_\infty}{I}\right)\frac{1}{\frac{dh}{d\phi}}$$

The experimental values of h/h_∞ were plotted in Fig. 7 against z/z_o and compared with the theoretical curve from Ref. 9. The agreement here is not as good as was obtained with the efficiency, but still appears reasonable.

The following general comments can be made concerning the correlation between the theory and the experimental points.

1. For helium and hydrogen, the experimental data indicate that the gas is heated more efficiently near the inlet than is predicted by the theory. This is not surprising, since it is near the cathode attachment point that the assumptions of the Stine-Watson theory would appear to be most unrealistic. In this region, the discharge channel diameter is probably much smaller than the diameter of the gas flow channel, hence the

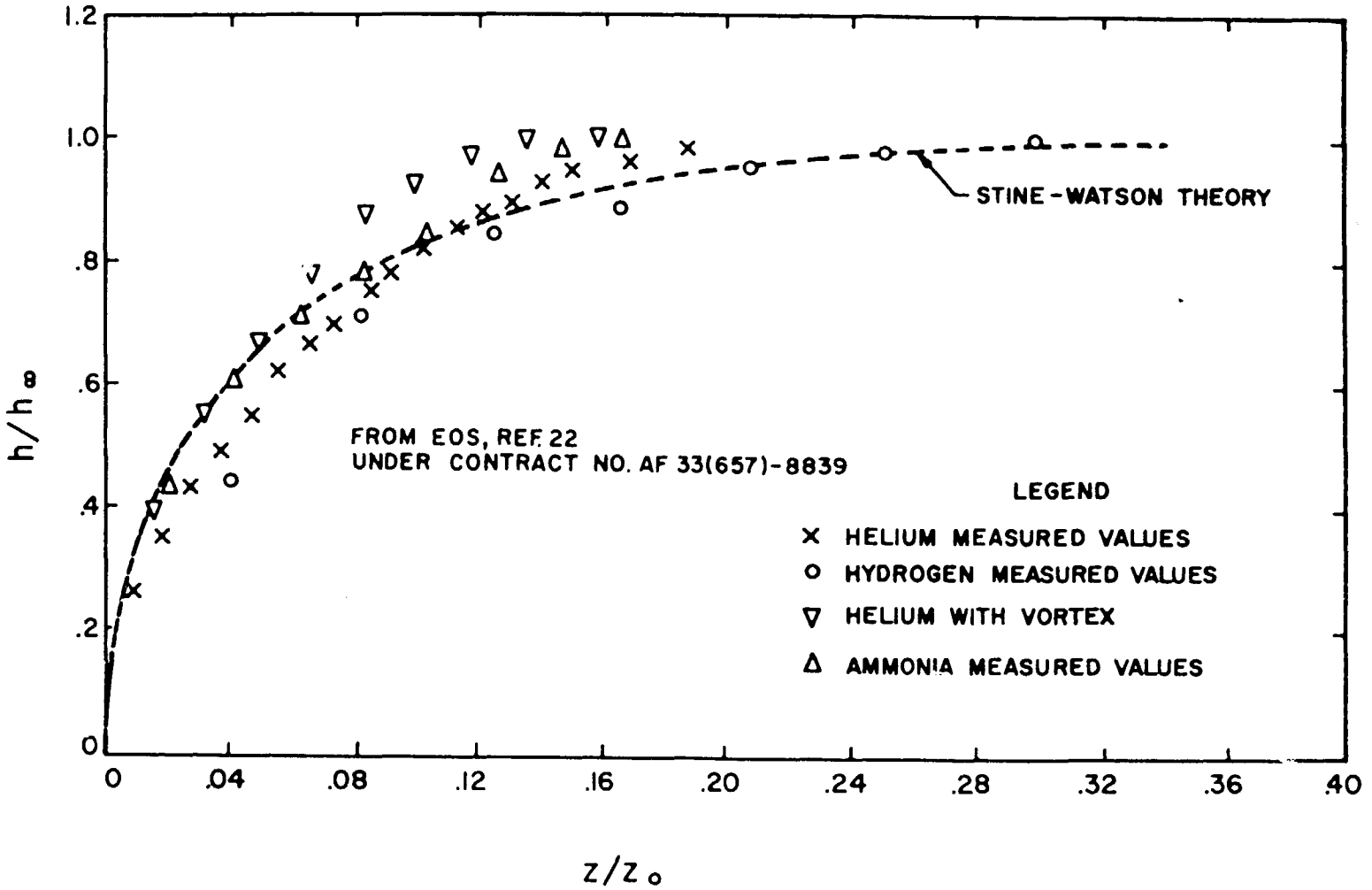

FIG. 7 COMPARISON OF GAS HEATING RATE IN ARC COLUMN WITH THEORETICAL VALUES

gas would be absorbing almost all of the electrical power from the discharge. This would account for a higher efficiency at the inlet than predicted by this simple theory.

2. For hydrogen, where σ vs. ϕ and h vs. ϕ curves were available, the values of $\frac{d\sigma}{d\phi}$ and $\frac{dh}{d\phi}$ which produced the fit to the data are not far from those one would read off the hydrogen curves. The differences are well within the expected accuracy of this very simple theoretical model.

3. The semi-empirical (i.e., "fitted") Stine-Watson curves (i.e., Figs. 6 and 7) seem to approximate the measured trends for engineering purposes.

3. PHYSICAL TRENDS AND CONCEPTS

3.1 Physical Processes

In a survey (Ref. 11) of nitrogen and air arc heaters, it was found that the performance limits achieved by many different development groups, using widely different geometrical configurations, all seemed to fall onto a fairly distinct band on the pressure-enthalpy map. This reaffirms our intuitive belief that all the more promising arc heater design approaches must, in the end, run into the same physical or technical limitations. Hence the "State of the Art Envelope", if it is meaningful, must be closely related to these technical limitations. Naturally we wish to understand this connection and find out how closely the present designs approach what might be considered "absolute" technical limits, with known materials and techniques. This would give us an indication of how much "room for improvement" we should expect to exist without a breakthrough or discovery of an entirely new and different approach.

The following physical mechanisms are likely to limit the ultimate obtainable performance of arc heaters:

The hot gas containment limits, imposed by conduction or convection and radiation heat transfer and the highest allowable wall heat loads of the containing vessel.

The heat retention problem of the gas, i.e., the allowable residence time of the heated gas vs. the time (volume) required for gas relaxation and mixing.

The electrode surface problems, i.e., the accommodation of the extreme local transient heat loads due to cathode and anode arc contractions (spot formation), in addition to the high mean arc chamber heat load. These three physical concepts are intimately related to the performance limits of all arc gas heaters. There are other important problem areas to be considered, but these do not suggest obvious physical limits to the potential gas heater performance.

In this report we intend to discuss only the hot gas containment limits. Further, we will confine the study to a configuration in which the gas flows axially through an axisymmetric electric discharge.

The physical quantities that will tend to cause limits on the map of enthalpy vs. pressure are heat conduction, "magnetic" pressure, radiation from the gas, and the dimensions of the arc heater. At the pressures and temperatures of interest, complete electromagnetic gas containment appears out of the question. Consequently, the walls of the containing vessel must withstand the full conductive (or convective) heat loads as well as that imposed by radiation from the gas. The following simple considerations will indicate the general trends and orders of magnitude involved.

In the arc heater or mixing chamber, the gas enthalpy distribution will be very roughly parabolic near the center and logarithmic near the walls. Radiation and turbulence will tend to flatten the enthalpy profile near the center, a thin arc filament along the centerline may steepen it a little, but by and large the profile will tend to return to its stable shape dictated by heat conduction.

If the mean gas enthalpy in the container $\bar{H}_t$ is given and if the dimensionless profile (h/h_w vs r/R) is assumed independent of the size, then it is evident that the wall heat flux due to conduction and convection will be proportional to the mean enthalpy and inversely proportional to the vessel size:

$$q_{con} \propto \frac{\bar{H}_t}{R}$$

The radiation intensity per unit volume, P_r, will, for the region of interest here, be roughly proportional to the electric conductivity (or the enthalpy above a certain level) and to the pressure. Outside of the luminous or conductive region the radiation will be close to zero. For an optically thin gas, all the radiation strikes the wall and is eventually absorbed by the wall, even if there are several reflections. For similar enthalpy profiles, the amount radiated increases as R^2, or the wall heat flux due to radiation increases like R.

$$q_{rad} \propto P_r R \; f(\bar{H}_t \text{ and shape of h distrib.})$$

As the heater size and pressure are increased, the radius eventually can become large compared with the optical path length and the radiation flux no longer increases with the heater size (grey gas approximation). Certainly

q_{rad} will never reach or exceed the black body intensity corresponding to the peak temperature in the center of the chamber. The total heat flux on the container wall is the sum of the convective and radiative contributions

$$q_w = q_{con} + q_{rad}$$

$$\sim k_c \frac{\bar{H}_t}{R} + k_R P_r R f(\bar{H}_t)$$

Clearly, for very small chambers and low pressures the conduction term will dominate, while for large chambers and high pressures q_{rad} will dominate. In the region where the gas is optically thin there will be a "best size" chamber for each pressure and enthalpy, that which makes the wall heat flux a local minimum. Conversely for each pressure there will be a highest enthalpy which can be accommodated within a given wall heat load (say $\sim$ 10 kw/cm^2). This will furnish one pressure-enthalpy containment limit, assuming that the "best size" can be used.

It is possible that for extremely large chamber sizes, in the grey gas radiation regime, still higher mean enthalpies are possible because there the wall does not "see" the hottest gas in the center. However, this is likely to occur outside of the practical size range of the tunnel heater, since this size is limited by other considerations. Thus the containment limit for any allowable q_w gives us a first limiting line on the pressure enthalpy map, at least for chamber sizes within the optically thin gas regime. At the same time this limit, if we have to approach it closely, prescribes approximate optimum chamber sizes for each pressure.

When the arc current is raised to large values, the radial forces in the discharge will tend to increase the average pressure in the heating column above the value at the wall. This effect imposes another constraint upon the heater and we expect that it will result in another pressure-enthalpy containment limit that the average gas pressure cannot fall below certain values which are dependent upon the average gas enthalpy.

An attempt is made in the following section of this paper to map out the attainable regions in the plot of enthalpy vs. pressure for air.

Some of the physical processes involved are described only in a very approximate manner in order to carry out this study. Despite this, the trends obtained are expected to be valid and the limiting values obtained to be correct to within a factor of better than 2.

3.2 Analytical Approach

A study of the containment limits for a hot gas resolves itself into attempts to solve the energy balance equation. When axial conduction and radial convection are neglected, the equation describing this balance can be written as follows:

$$\frac{\partial}{\partial z}(\rho w h) - \frac{1}{r}\frac{\partial}{\partial r}\left(r K \frac{\partial T}{\partial r}\right) + P_r = j^2/\sigma \qquad (1)$$

The quantities h, K, P_r, σ, are in general, all complicated functions of pressure and temperature. These transport properties have been computed by a number of investigators. One of the latest evaluations is that of Yos (Ref. 12). An estimate of the complexity of the relationships can be found from examining the data in Figs. 8, 9, 10, taken from Ref. 12, where K, σ and P_r for air are shown as a function of temperature and pressure. Clearly, no simple general solution to Eq. (1) can be obtained. Attempts to obtain approximate solutions for the energy balance in an arc have a long and colorful history. Many models have been postulated, and the results of each have some validity over restricted temperature and pressure regimes. A complete numerical integration of the equations is almost out of the question, hence models will be used to study arc heaters for some time to come. The need for realistic approximations is becoming increasingly important as theory and experiment are now being checked one against the other and theory is now being used to aid in the design of arc heaters.

For many years effort was concentrated on solving only the problem of the asymptotic arc, i.e., no gas is flowing through the arc or else the gas has been heated downstream to the point where $\frac{\partial}{\partial z}(\rho w h) = 0$. From studies of this kind it is possible to obtain unique relationships among the average gas enthalpy, the heat flux rate, the pressure, the arc

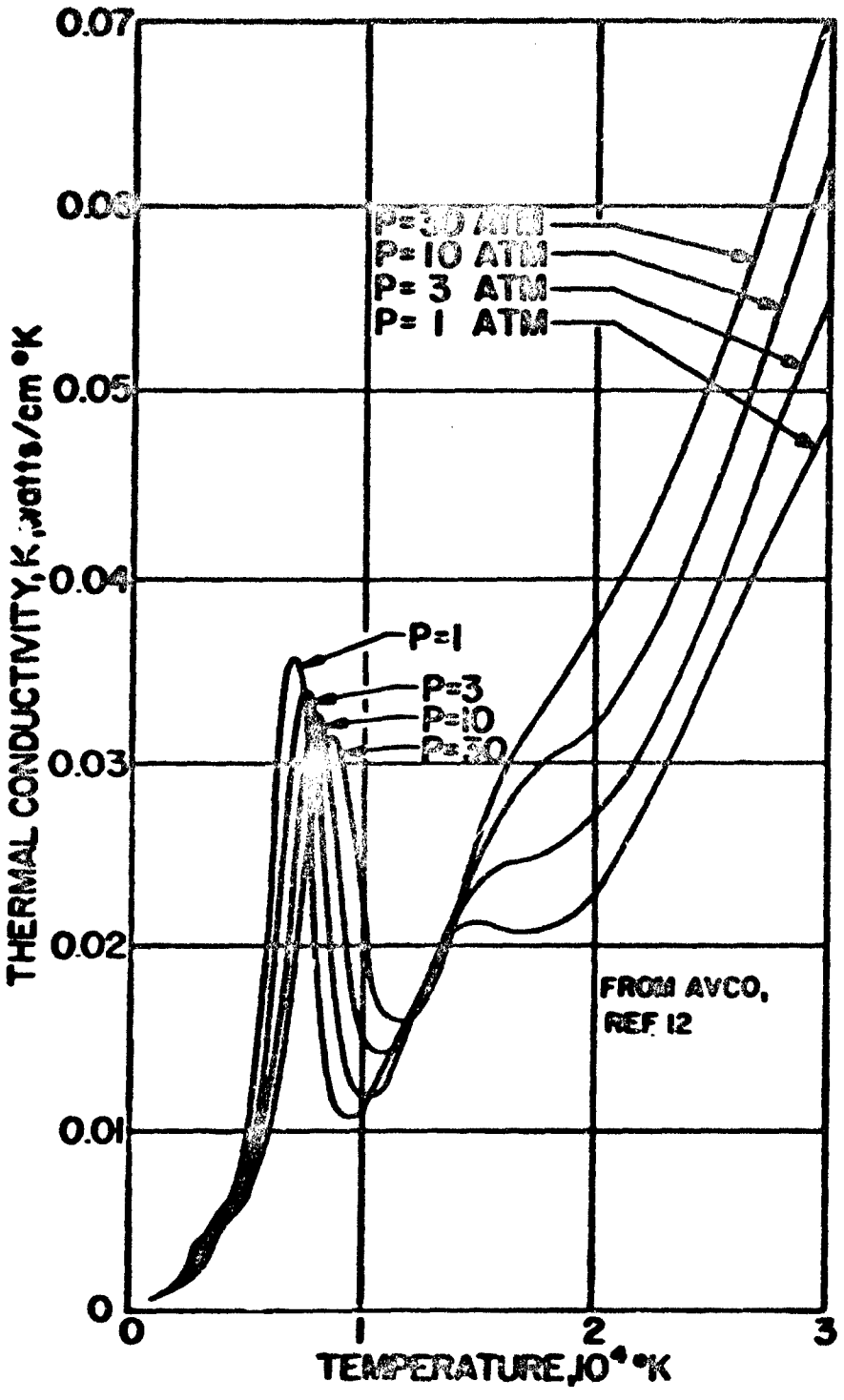

FIG. 8 THERMAL CONDUCTIVITY OF AIR VERSUS TEMPERATURE

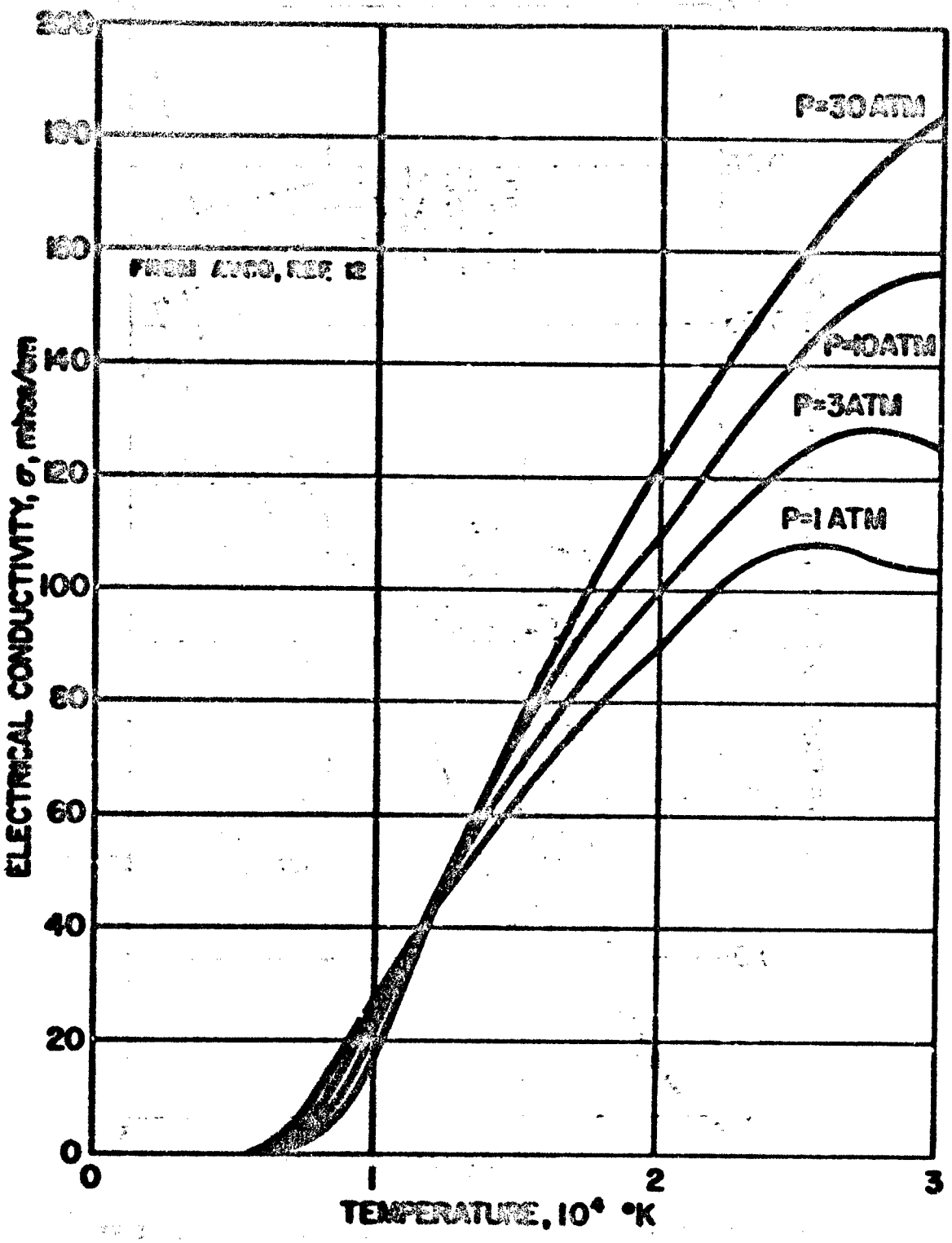

FIG. 9 ELECTRICAL CONDUCTIVITY OF AIR VERSUS TEMPERATURE

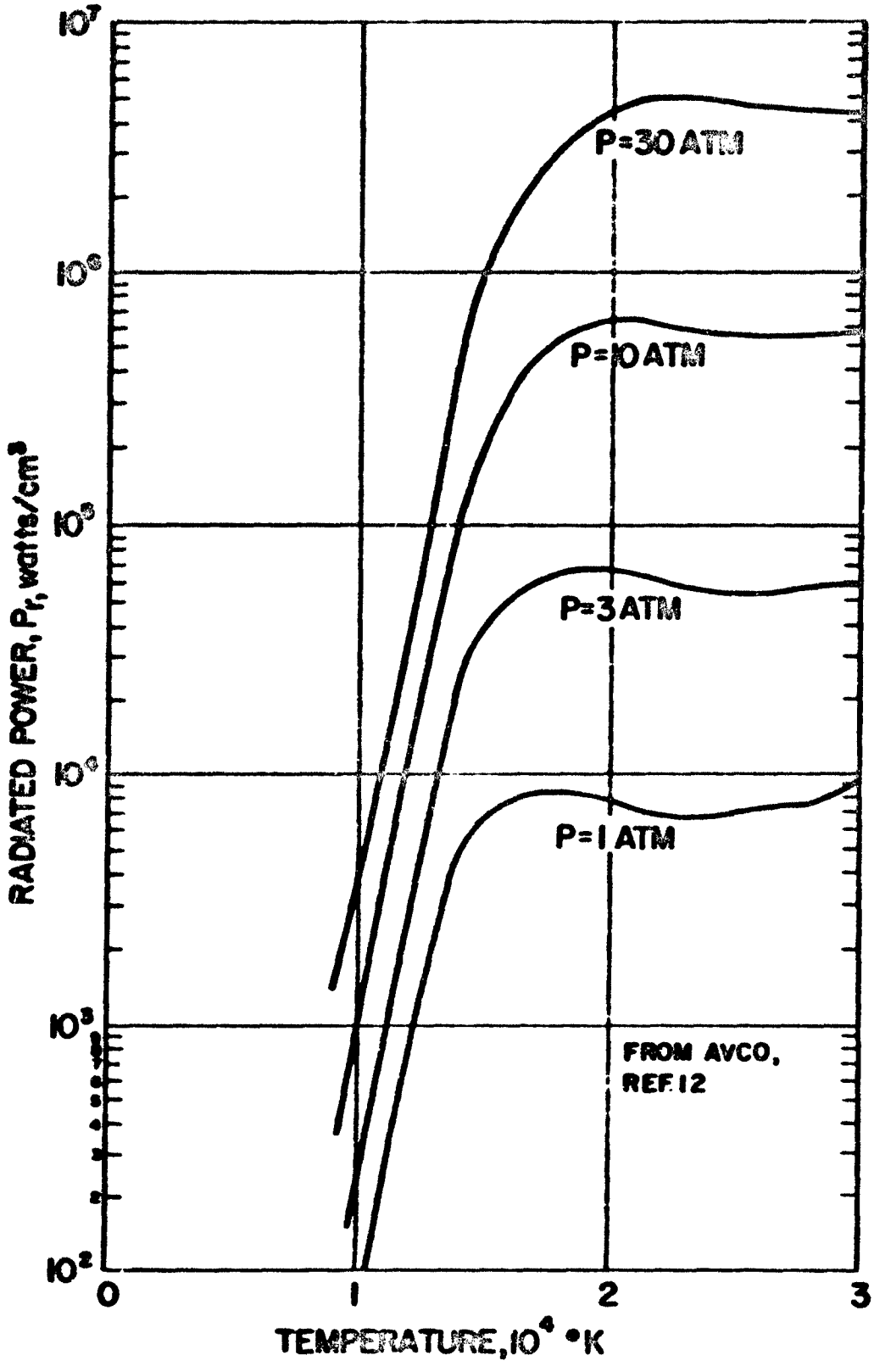

FIG. 10 CONTINUUM RADIATED POWER PER UNIT VOLUME FROM AIR VERSUS TEMPERATURE

current, the arc radius and the radius of the containing cylinder. This is adequate for determining the ultimate performance capability of arc heaters. Also, correlations between theory and experiment are best made in this region, when it is possible to use the theory and measurements to determine the electrical and thermal conductivity of the gas.

When more information about the heating process is required, it is necessary to solve Eq. (1) completely. This solution supplies the additional information of the heater length, the efficiency of the heating process and the voltage that must be applied across the heater. In order to obtain analytic solutions in the heating region, it is necessary to have the radial profiles "similar" at each axial position. This restriction makes the solutions somewhat unrealistic near the heater inlet, hence the initial heating of the gas as it enters the arc is probably not described too well. In general, this is not a serious objection to the theory, since no critical problem in heater performance occurs here.

The first major breakthrough in the technique of handling this equation in the regime where $\frac{\partial}{\partial z}_T (\rho w h) = 0$ (asymptotic regime) resulted from introducing a new variable $\phi = \int_0 K\, dT$, instead of using the temperature itself. This greatly simplified the determination of the radial temperature profiles. Once this was done, progress in obtaining solutions to the more general problem of the rate of heating of the gas has been rapid. One of the most useful approximations in solving this problem has been found to be

$$h - h_1 = \frac{dh}{d\phi} (\phi - \phi_1)$$

where $\frac{dh}{d\phi}$ is independent of pressure. A plot of $h - h_1$ vs. $\phi - \phi_1$ is shown in Fig. 11 for nitrogen and the linear approximation is shown to be quite good. To a first approximation, $\frac{dh}{d\phi}$ is also seen to be independent of pressure. It should be noted that this quantity is the ratio of the specific heat of the gas at constant pressure to the thermal conductivity:

$$\frac{dh}{d\phi} = \frac{C_P}{K}$$

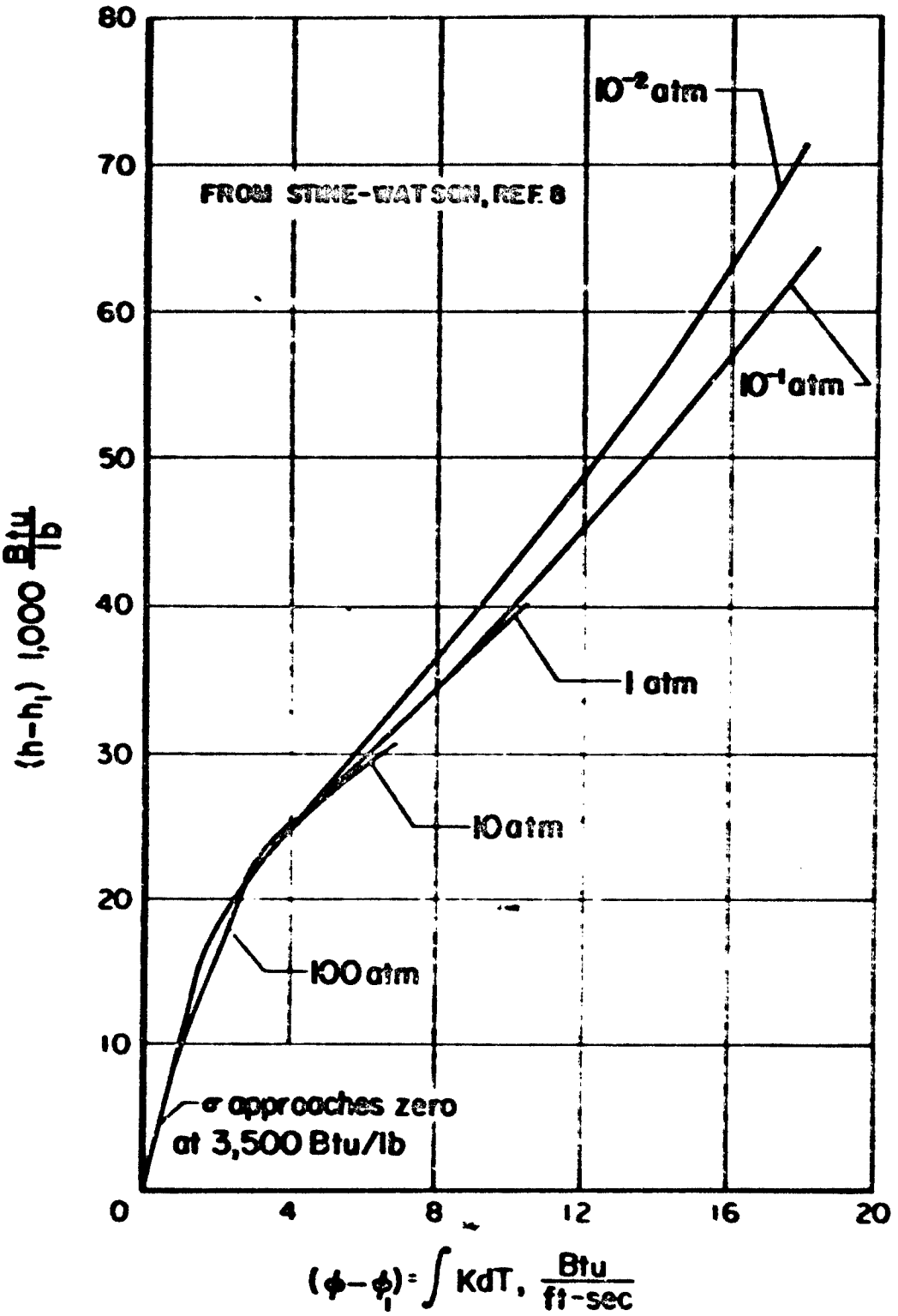

FIG. 11 RELATIONSHIP BETWEEN ENTHALPY AND CONDUCTION FUNCTION FOR AIR IN THERMODYNAMIC EQUILIBRIUM

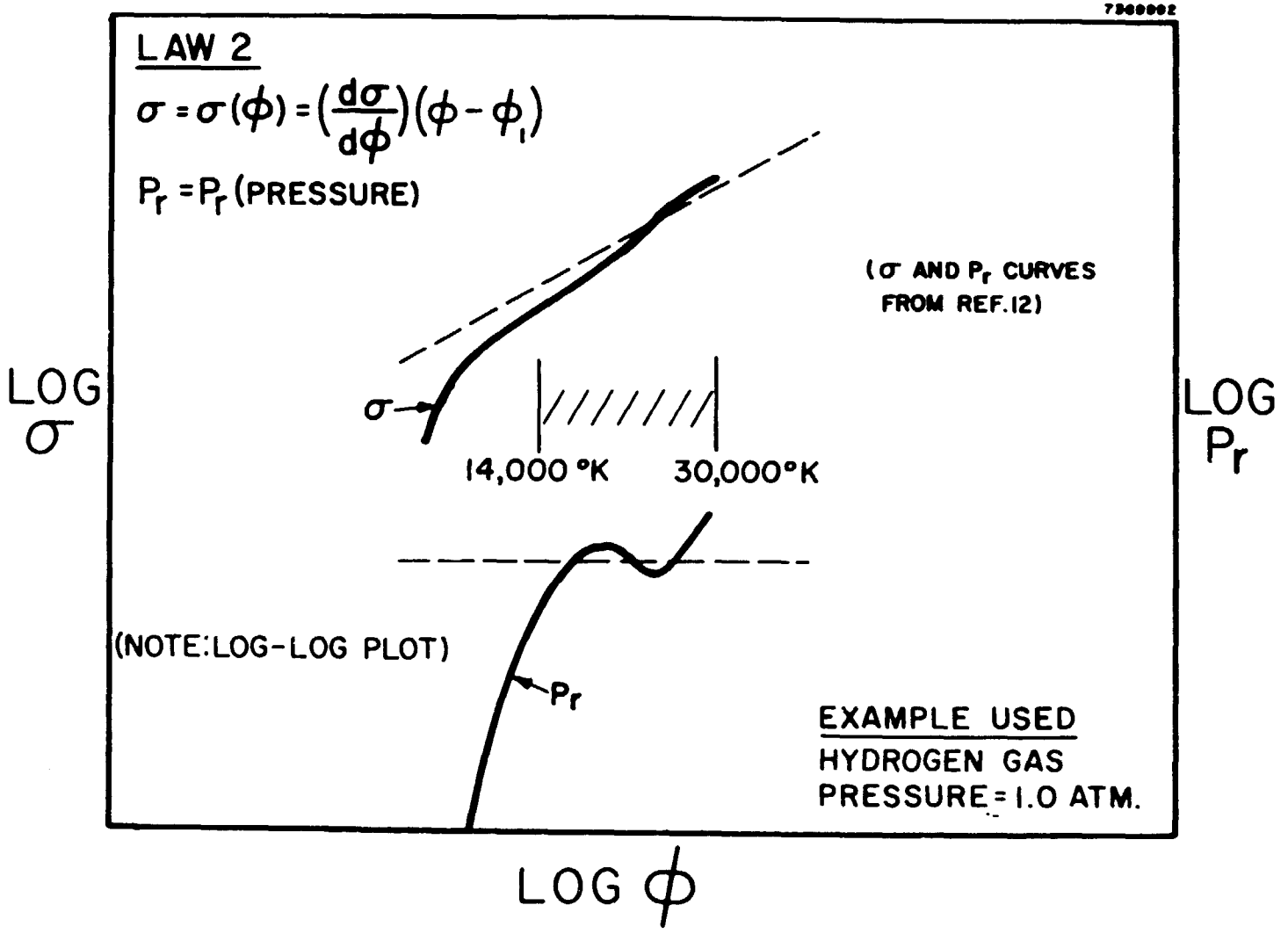

FIG. 13 COMBINATION OF LINEAR AND CONSTANT APPROXIMATION FOR TRANSPORT COEFFICIENTS

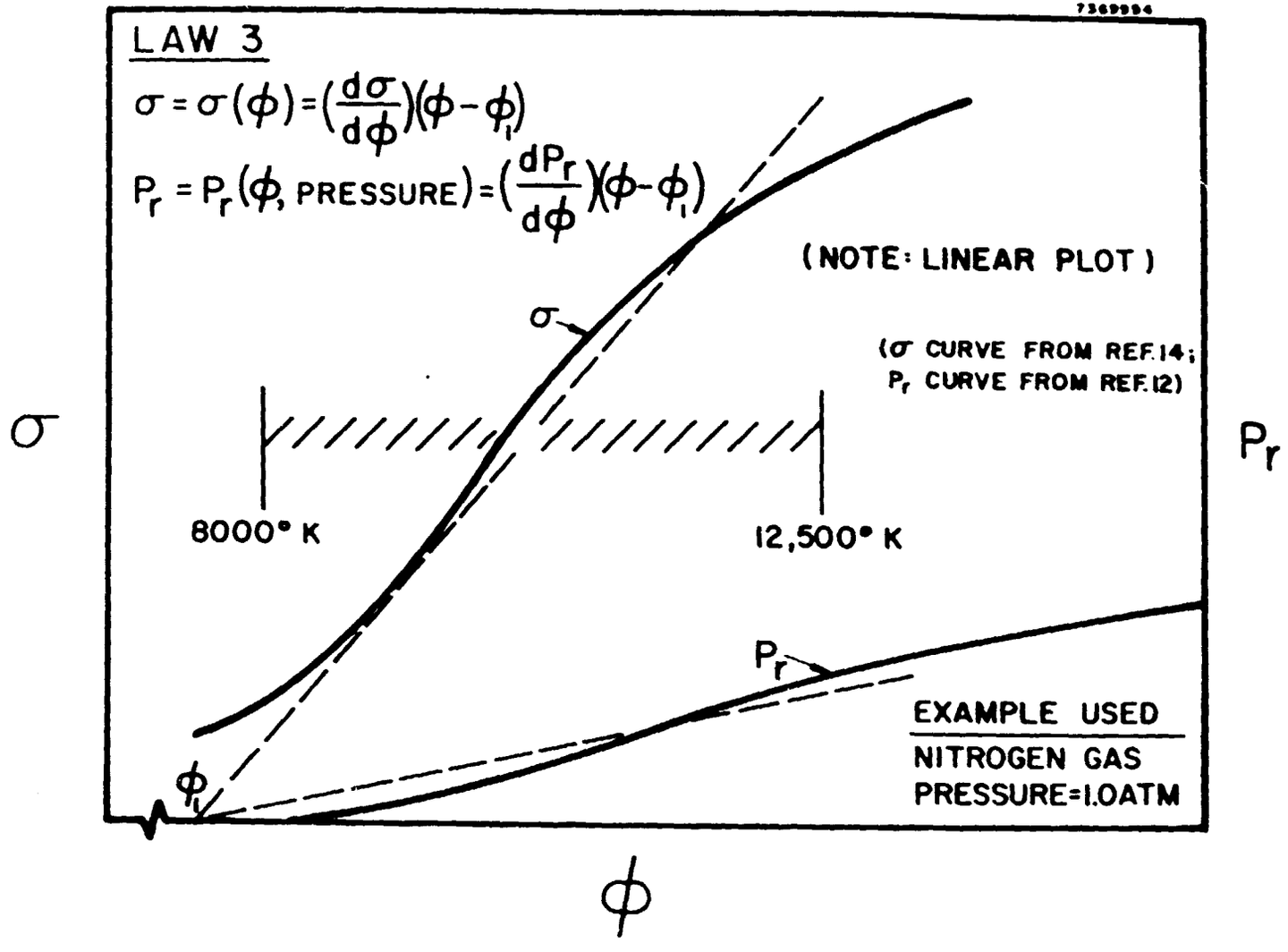

FIG. 14 LINEAR APPROXIMATION FOR TRANSPORT COEFFICIENTS

Various relations among ϕ, σ, and P_r exist over restricted ranges of temperature for different gases. Some idea of the approximations used and of their validity can be obtained by examining Figs. 12, 13, and 14. Here the electrical conductivity σ and the power radiated per unit volume P_r is plotted vs the thermal conductivity integral for several gases. An attempt is made to obtain a straight line approximation between σ or P_r and ϕ in all cases for a given pressure. In almost all cases it is assumed that the electrical conductivity is independent of the pressure. When this is done, the only quantity which introduces the pressure into the analysis is the radiated power per unit volume P_r. An attempt was made to list which cases have been studied and who the investigator was in Table I.

One of the aims of this paper is to map out the physically attainable regimes on the enthalpy-pressure map. For this purpose, solutions to Eq. (1) in the asymptotic regime are adequate. Accordingly, two solutions to the problem are presented in the following section for two different approximations for the relations among the thermal conduction integral ϕ, the electrical conductivity of the gas σ, and the radiated power per unit volume from the gas P_r.

THEORETICAL TREATMENT OF THE COAXIAL FLOW DISCHARGE

TABLE I - ABBREVIATED LITERATURE GUIDE

ANALYTICAL APPROACH USED	INVESTIGATORS AND REFERENCES
I. Asymptotic (Fully Developed) Constricted Arc Column*	
A. Model Theories Without Radiation a) σ assumed function of T or of ϕ b) σ or T or ϕ assumed function of radius	Classical Problem, many papers since ~ 1930 Summaries: Uhlenbusch (3), Maecker (4) Peters (15), Chen (5), Buhler (2), Skifstad (16)
B. Model Theories With Radiation a) σ and P_r assumed functions of T or of ϕ	Maecker (17), Uhlenbusch (3), Present Paper
C. Model Theories With Radiation and Magnetic Pressure	Present Paper
D. Numerical Integrations (Iteration Solutions) Using "exact" (i.e. the best available) material function curves, some without and some with radiation	Brinkman (18), Koch, Lesemann and Walther (19), King (20), Uhlenbusch (3), Schmitz, Patt and Uhlenbusch (4), Marlotte (21)
II. Inlet or Heating Region	
A. Model Theory Without Radiation. σ, and h assumed as linear functions of ϕ	Stine and Watson (8)
B. Model Theory With Radiation. σ, h and P_r assumed as linear functions of ϕ	Present Paper
C. Other Approximate Analyses	Cassie (7), John, Chen, et al (10), Skifstad and Murthey (9)

*Note: This list covers primarily treatments of the "direct" problem, where the material functions are considered as known functions of the temperature, and the arc voltage and the temperature distribution are the unknowns. Many other arc studies deal with the "inverse" problem in which the material functions are to be calculated from arc measurements.

4. ANALYSIS

4.1 Low Enthalpy Solution for Air Arc Heaters

When the air temperature is below 15,000 ^{o}K, the gas transport properties can be approximated reasonably well by the following relations:

$$h - h_1 = \frac{dh}{d\phi}(\phi - \phi_1) \tag{2}$$

$$P_r = \left(\frac{dP_r}{d\phi}\right)_a \left(\frac{p}{p_a}\right)(\phi - \phi_1) \tag{3}$$

$$\sigma = \frac{d\sigma}{d\phi}(\phi - \phi_1) \tag{4}$$

The subscript "a" refers to atmospheric pressure as a reference. The subscript 1 logically refers to that enthalpy or gas temperature at which the electron density becomes negligible. This point is, however, usually determined by extrapolating the straight line approximations between ϕ and σ and between ϕ and P_r to the ϕ axis and ensuring that the same value of ϕ_1 is obtained from the two lines. When these values are inserted into the energy balance equation a solution is obtained for the case when $\frac{\partial}{\partial z}(\rho w h) = 0$.

The solution for the radially-averaged gas enthalpy can be written as follows:

$$h_{avg} - h_1 = \frac{2.4\,\frac{dh}{d\phi}\,I\left[\left(\frac{r_1}{2.4}\right)^2 - \frac{R^2}{2}\ln\frac{R}{r_1} + \frac{R^2 - r_1^2}{4}\right]}{\pi R^2 r_1 \left(\frac{d\sigma}{d\phi}\right)^{1/2}\left[1 + \left(\frac{r_1}{2.4}\right)^2 \left(\frac{dP_r}{d\phi}\right)_a \frac{p}{p_a}\right]^{1/2}} \tag{5}$$

In this expression, r_1 represents the outer radius of the arc and R represents the wall radius. The wall heat load which now includes the radiation and conduction heat flux can be written as:

$$q_w = \frac{2.4I\left[1 + \left(\frac{r_1}{2.4}\right)^2 \left(\frac{dP_r}{d\phi}\right)_a \left(\frac{p}{p_a}\right)\right]^{1/2} \frac{r_1}{R}}{2\pi r_1^2 \left(\frac{d\sigma}{d\phi}\right)^{1/2}} \tag{6}$$

When $p \to 0$, these two expressions reduce to the value found by Stine and Watson in Ref. 8 , for the average gas enthalpy and wall heat load. For a fixed wall radius and arc current, it is apparent that the radiation heat load increases the wall heat load and decreases the gas enthalpy. A rather simple relation exists between the average gas enthalpy and the wall heat load:

$$\frac{h_{avg} - h_1}{q_w} = \frac{2\frac{dh}{d\phi}\left[\left(\frac{r_1}{2.4}\right)^2 - \frac{R^2}{2}\ln\frac{R}{r_1} + \frac{R^2 - r_1^2}{4}\right]}{R\left[1 + \left(\frac{r_1}{2.4}\right)^2\left(\frac{dP_r}{d\phi}\right)_a \frac{p}{p_a}\right]} \tag{7}$$

A similar expression can be found for the gas in the region between the arc and the wall:

$$\frac{h_w - h_1}{q_w} = \frac{-R\frac{dh}{d\phi}\ln\frac{R}{r_1}}{\left[1 + \left(\frac{r_1}{2.4}\right)^2\left(\frac{dP_r}{d\phi}\right)_a \frac{p}{p_a}\right]} \tag{8}$$

At this point it is desirable to determine if some check can be made of the validity of the technique by which the radiation was introduced into the analysis. Accordingly, the radiation per unit length from an argon arc was determined using the equipment described in Sec. 2. Measurements were made at currents of 100, 180, 200, and 210 amperes, and the ambient pressure was maintained at one atmosphere. The data from these experiments is plotted in Fig. 15. An expression for the radiated power per unit length of arc as a function of arc current can be found from the theory outlined above.

$$\frac{P_{rad}}{L} = \frac{2.4}{r_1}\frac{I}{\left(\frac{d\sigma}{d\phi}\right)^{1/2}}\frac{\left(\frac{r_1}{2.4}\right)^2\left(\frac{dP_r}{d\phi}\right)_a \frac{p}{p_a}}{\left[1 + \left(\frac{r_1}{2.4}\right)^2\left(\frac{dP_r}{d\phi}\right)\frac{p}{p_a}\right]^{1/2}} \tag{9}$$

The value of the arc radius r_1 determined from the following relation

$$\frac{\phi_1 - \phi_w}{q_w} = \frac{R \ln R/r_1}{\left[1 + \left(\frac{r_1}{2.4}\right)^2\left(\frac{dP_r}{d\phi}\right)_a \frac{p}{p_a}\right]} \tag{10}$$

where q_w is calculated from the measured power absorbed by a segment. Over the current range of 100 to 250 amperes, it was found that $r_1 \approx R$ now in the

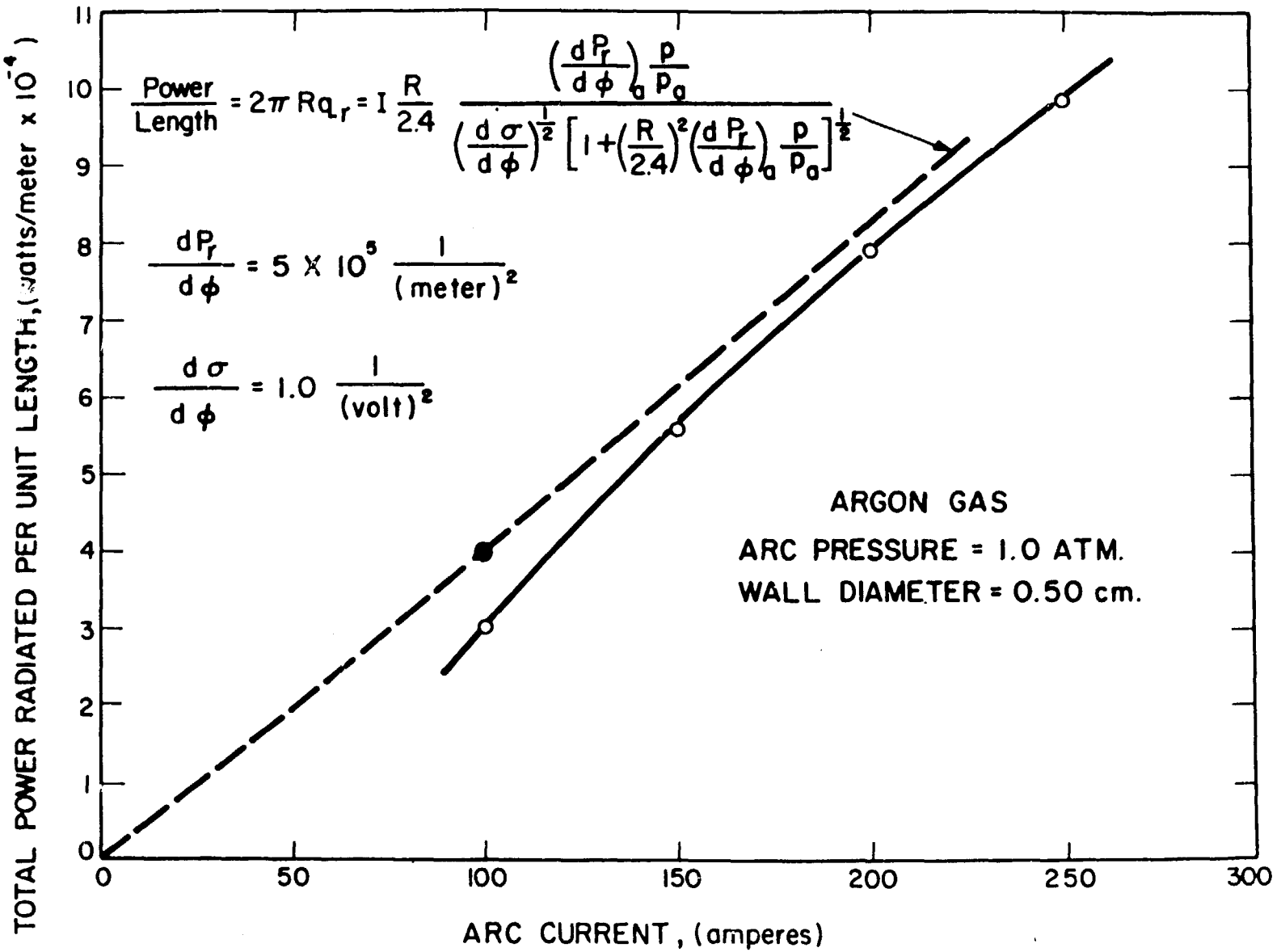

FIG. 15 RADIATION INTENSITY VERSUS CURRENT FOR SEGMENTED COLUMN EXPERIMENT

Eq.(9) fo. the radiated power per unit length and we obtain

$$\frac{P_{rad}}{L} = \frac{I}{\left(\frac{d\sigma}{d\phi}\right)^{1/2}} \frac{\frac{R}{2.4}\left(\frac{dP_r}{d\phi}\right)_a \frac{p}{p_a}}{\left\{1 + \left(\frac{R}{2.4}\right)^2 \left(\frac{dP_r}{d\phi}\right)_a \frac{p}{p_a}\right\}^{1/2}} \qquad (11)$$

From the argon transport properties evaluated by Baum and Marlotte at EOS, the values of $\left(\frac{d\sigma}{d\phi}\right)^{1/2}$ and $\left(\frac{dP_r}{d\phi}\right)_a$ are found to be

$$\left(\frac{dP_r}{d\phi}\right)_a = 5 \times 10^5 \ \frac{1}{\text{meter}^2}$$

$$\frac{d\sigma}{d\phi} = 1.0 \ \frac{1}{\text{volt}^2}$$

Using these values, the theoretical line shown on Fig. 15 was drawn in. The theoretically predicted curves agree with the measured data for the radiated power to within about ±20%. More important, the predicted dependence of radiation upon arc current is shown to be reasonably in agreement with experiment.

The experimental and theoretical agreement on the radiation from the arc, combined with the correlations found in Sec. 2 for the gas heating rate in the constricted arc, now give us confidence in using the theory to predict the ultimate performance capability of arc heaters based upon the criterion that the wall heat flux rate at the outlet end of the constrictor is the critical heat load in the device. Considerable ingenuity is required in electrode design to insure that they do not burn out before the constrictor does, but this can probably be accomplished.

A maximizing procedure to determine the highest radially-averaged gas enthalpy attainable at a given gas pressure can now be carried out using the theoretical equations derived above. The gas pressure, p/p_a, the gas enthalpy at the wall, h_w, the gas enthalpy at the edge of the discharge h_1, and the wall heat flux rate will be held fixed. The value of wall radius R that maximizes the average gas enthalpy is then solved for, from Eq. (7) subject to the restriction imposed by Eqs. (6, 10). When this is done it is found that the condition for the maximum enthalpy occurs when the wall heat load is equally divided between conduction and radiation. The complete solution for the optimum heater performance can be written in parametric form as follows:

$$\frac{(h_1 - h_w)^2 \left(\frac{dP_r}{d\phi}\right)_a}{(2.4)^2 \left(\frac{dh}{d\phi}\right)^2 q_w^2} \quad \frac{p}{p_a} = \left(\frac{1}{2} \frac{R}{r_1} \ln \frac{R}{r_1}\right)^2 \tag{12}$$

$$\frac{h_{avg} - h_1}{h_1 - h_w} = \frac{\left(\frac{2}{2.4}\right)^2 + \left(\frac{R}{r_1}\right)^2 - 2\left(\frac{R}{r_1}\right)^2 \ln \frac{R}{r_1} - 1}{2\left(\frac{R}{r_1}\right)^2 \ln \frac{R}{r_1}} \tag{13}$$

$$\frac{\frac{dh}{d\phi} q_w}{h_1 - h_w} R = \frac{2}{\ln \frac{R}{r_1}} \tag{14}$$

$$\frac{2.4\sqrt{2}}{2\pi} \quad \frac{\left(\frac{dh}{d\phi}\right)^2 q_w}{\left(h_1 - h_w\right)^2 \left(\frac{d\sigma}{d\phi}\right)^{1/2}} I = \frac{4}{\frac{R}{r_1} \ln\left(\frac{R}{r_1}\right)^2} \tag{15}$$

The expressions appearing on the left sides of these equations can be expressed in terms of more familiar non-dimensional numbers.

$$\frac{\frac{dh}{d\phi} q_w R}{h_1 - h_w} = \frac{C_p q_w R}{K (h_1 - h_w)} = \frac{\text{total heat load}}{\text{conductive heat load}} \tag{16}$$

$$= \text{Nusselt number} = Nu$$

$$\frac{\left(h_1 - h_w\right)^2 \left(\frac{dP_r}{d\phi}\right)_a}{2.4^2 \left(\frac{dh}{d\phi}\right)^2 q_w^2} = \frac{1}{(Nu)^2} \left(\frac{R}{2.4}\right)^2 \left(\frac{dP_r}{d\phi}\right)_a \tag{17}$$

where

$$\left(\frac{R}{2.4}\right)^2 \left(\frac{dP_r}{d\phi}\right)_a = \frac{\text{radiation heat flux}}{\text{conductive heat flux}}$$

$$\frac{2.4\sqrt{2}}{2\pi} \frac{\left(\frac{dh}{d\phi}\right)^2 q_w I}{\left(h_1 - h_w\right)^2 \left(\frac{d\sigma}{d\phi}\right)^{1/2}} = Nu^2 \left\{ \frac{2p}{\mu_o \frac{d\sigma}{d\phi} q_w^2 \left(\frac{R}{2.4}\right)^2} \frac{\mu_o I^2}{4\pi^2 R^2 p} \right\}^{1/2} \tag{18}$$

where

$$\frac{\mu_o \frac{d\sigma}{d\phi} q_w^2 \left(\frac{R}{2.4}\right)^2}{2p} = \frac{\text{mass transport diffusivity}}{\text{magnetic diffusivity}}$$

$$= \text{magnetic Reynold's number}$$

and where

$$\frac{\mu_o I^2}{4\pi^2 R^2 p} = \frac{\text{magnetic pressure}}{\text{static gas pressure}}$$

$$= \text{magnetic pressure number}$$

By assigning values to $\frac{R}{r_1}$ of from unity to infinity, relations can be found among the four quantities on the right of these equations. Values can then be assigned to the constants and relations found among the pressure in the gas, the average gas enthalpy, the arc current and the radius of the arc heating cylinder or constrictor. The following values were determined for the constants for air from Refs. (8, 3).

$$\frac{dh}{d\phi} = 5.37 \times 10^3 \quad \frac{\text{meter-sec}}{\text{kgm}}$$

$$\frac{d\sigma}{d\phi} = .642 \quad \frac{1}{\text{volts}^2}$$

$$\frac{dP_r}{d\phi}_a = 1.00 \times 10^5 \quad \frac{1}{\text{meter}^2}$$

$$\frac{h_1}{RT_o} = 100$$

$$\frac{h_w}{RT_o} = 13$$

$$RT_o = 7.87 \times 10^4 \quad \frac{\text{meters}^2}{\text{sec}^2}$$

$$p_a = 1.01 \times 10^5 \quad \frac{\text{newtons}}{\text{meter}^2}$$

Using these values, for each assigned wall heat flux rate, q_w, it is possible to establish a curve in the plane of $\frac{h_{avg}}{RT_o}$ versus $\frac{p}{p_a}$. The arc current, constrictor radius and power in the gas can also be established at each point along this curve. Accordingly, the lower sections of Figs. 16, 17, and 18, where the linear approximations of Eqs. 2, 3, and 4 may be expected to be valid, were calculated and drawn in. Theory and experiment have established that 10^8 watts/meter^2 or 10 kw/cm^2 is near the maximum heat transfer rate that can be conducted through a metal without melting the surface. Heat loads of this value have been obtained with water cooled copper where the heat load was produced by an arc. The curves for lower values of q_w

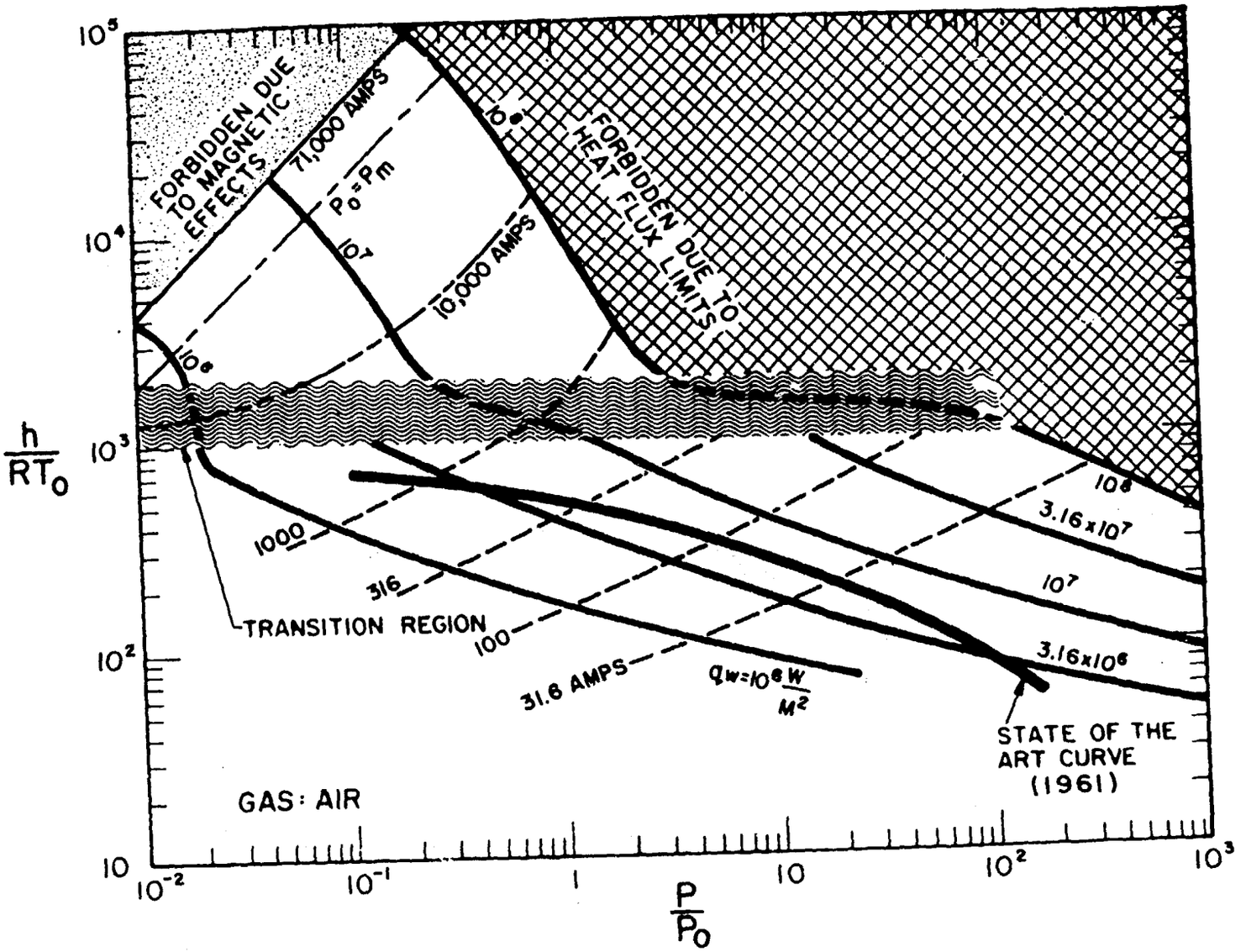

FIG. 16 CONTAINMENT LIMITS FOR AIR ARC HEATERS; LINES OF CONSTANT CURRENT

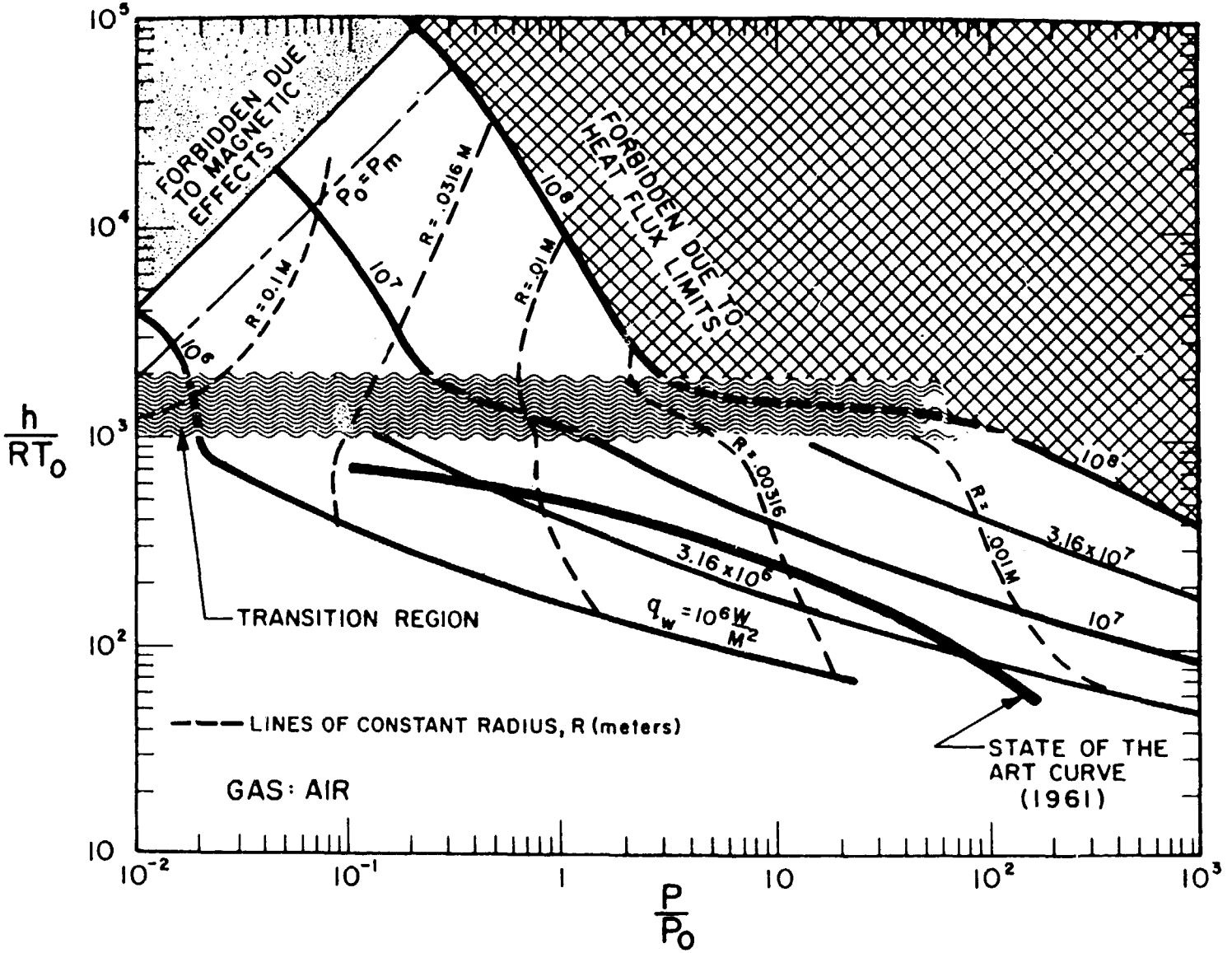

FIG. 17 CONTAINMENT LIMITS FOR AIR ARC HEATERS; LINES OF CONSTANT RADIUS

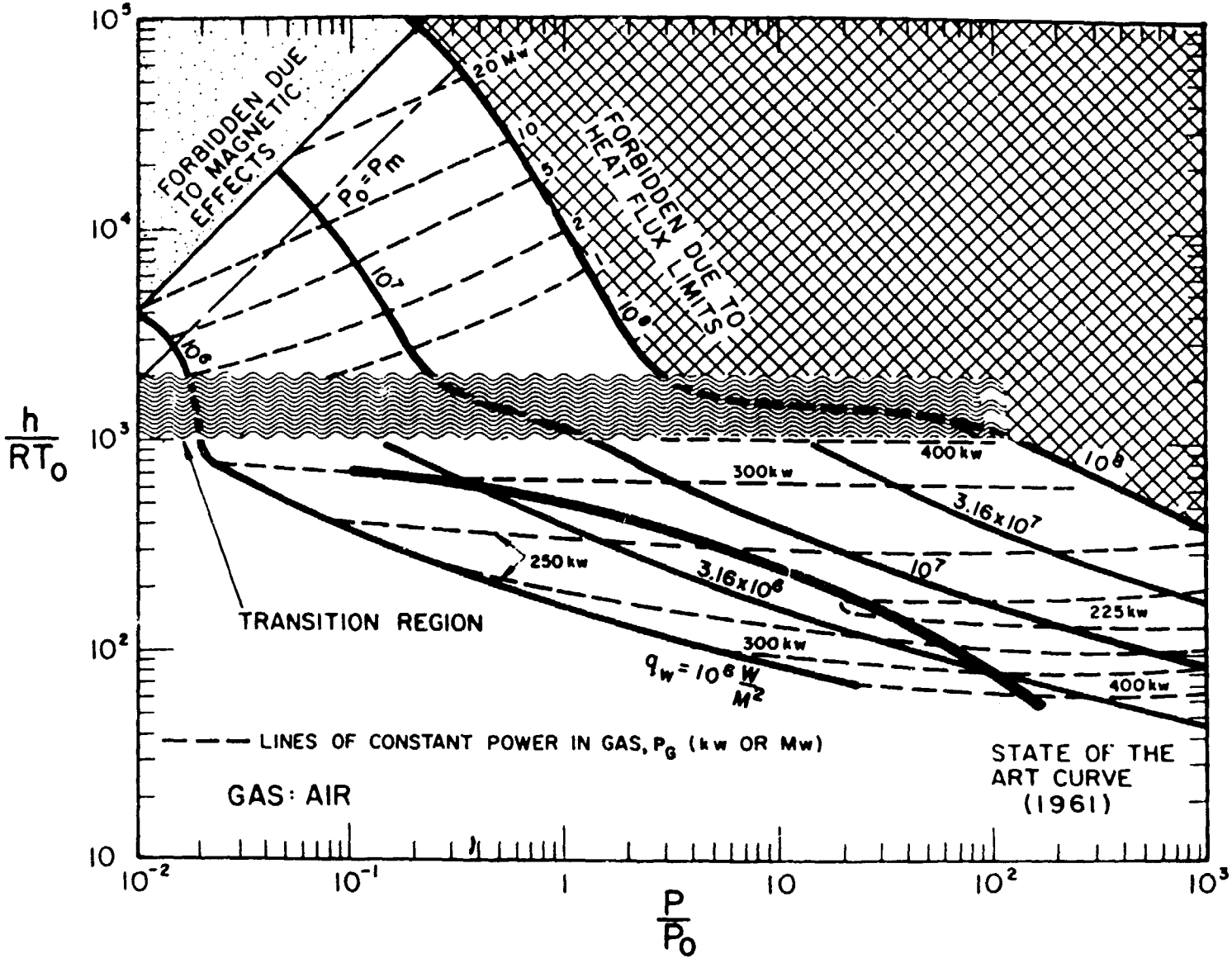

FIG. 18 CONTAINMENT LIMITS FOR AIR ARC HEATERS; LINES OF CONSTANT POWER IN THE GAS

establish how the performance capability of the arc heater is degraded when the constrictor components are not cooled as well as they might be.

The data established from this evaluation are expected to be valid up to temperatures of about 15,000 ^{o}K for the gas, or enthalpies of about $\frac{h}{RT_o} \approx 1000$. For enthalpies above this value, other approximations for the relations among the thermal conduction integral ϕ, the radiated power per unit volume P_r and the electrical conductivity σ must be used.

4.2 High Enthalpy Solution for Air Arc Heaters

The transport properties of high temperature air ($T > 15,000$ ^{o}K) are quite different than those for low temperature air and can be described approximately by the following relations:

$$h - h_1 = \frac{dh}{d\phi} (\phi - \phi_1) \tag{19}$$

$$P_r = \left(P_r \right)_a \left(\frac{p}{p_a} \right)^2 \tag{20}$$

$$\sigma = \sigma_a \tag{21}$$

The radiated power per unit volume is evaluated at atmospheric pressure, hence the subscript "a". The quantity h_1 is introduced to define a temperature at which the approximations for P_r and σ cease to ba valid.

As the arc current is increased and the gas pressure is reduced, it will no longer be possible to neglect the radial pressure gradient caused by the pinching forces of the arc current interacting with its own magnetic field. Since the radiated power per unit volume depends upon the local gas pressure, there will now be a strong interaction between the enthalpy distribution in the arc and the arc current. An expression for the radial distribution of pressure in the discharge can readily be found because of the assumption of constant electrical conductivity.

$$p = p_w + \frac{\mu_o I^2}{4\pi^2 r_1^4}\left(r_1^2 - r^2\right) \tag{22}$$

The further assumption is now made that $R \approx r_1$, or that the discharge fills the constrictor. This assumption will be checked later in order to determine the error introduced. The equation for the pressure now becomes

$$p = p_w + \frac{\mu_o I^2}{4\pi^2 R^4}(R^2 - r^2) \tag{23}$$

A solution to the energy balance equation can be found using the relations discussed above. Once again, only the solution when $\frac{\partial}{\partial z}(\rho w h) = 0$, will be discussed, although the general solution can be obtained. As in the previous case, it is possible to determine an arc radius for highest enthalpy when the pressure at the wall and the wall heat flux rate are held constant. The condition resulting from this optimizing procedure gives a ratio of the heat load due to radiation to the total heat load at the wall

$$\frac{q_{rad}}{q_w} = \frac{1}{2}\,\frac{1 + (R_e)_M + \frac{1}{3}(R_e)_M^2}{\left[1 + (R_e)_M\right]^2} \tag{24}$$

where $(R_e)_M = \dfrac{\mu_o \sigma q_w R}{p_w}$

For low values of the magnetic Reynold's number $(R_e)_M$, the heat load is found to divide equally between radiation and conduction. This agrees with the distribution found in the previous case, where it was tacitly assumed that $(R_e)_M \ll 1$. A set of parametric relations can now be found among the average gas pressure, the average gas enthalpy, the constrictor radius and the arc current.

$$(R_e)_M = \frac{\mu_o \sigma q_w R}{2 p_w}$$

$$\left[\frac{2 (P_r)_a p_a}{\mu_o \sigma q_w^2}\right]^{1/3} \frac{p_{av}}{p_a} = \left[1 + \frac{(R_e)_M}{2}\right] \frac{1}{\left[(R_e)_M \left[1 + (R_e)_M\right]^2\right]^{1/3}} \qquad (25)$$

$$\left[\frac{2(P_r)_a \mu_o^2 \sigma^2}{q_w^2 p_a^2}\right]^{1/3} \frac{h_{av}-h_1}{\frac{dh}{d\phi}} = \frac{(R_e)_M^2 \left[1 + \frac{8}{3}(R_e)_M + \frac{3}{2}(R_e)_M^2\right]}{4\left[(R_e)_M \left[1 + (R_e)_M\right]^2\right]^{4/3}} \qquad (26)$$

$$\left[\frac{2 (P_r)_a \mu_o^2 \sigma^2 q_w}{p_a^2}\right]^{1/3} R = 2\left[\frac{(R_e)_M}{1 + (R_e)_M}\right]^{2/3} \qquad (27)$$

$$\left[\frac{2 (P_r)_a \mu_o^2 \sigma}{4\pi^2 p_a^2}\right]^{1/2} I = 2 \frac{(R_e)_M}{1 + (R_e)_M} \qquad (28)$$

The expressions on the left of these equations can be written in terms of the four non-dimensional numbers found in the previous solution, with some slight modifications of definition. The values assigned to the various constants for air over 16,000 ^{o}K are listed below:

$$\frac{dh}{d\phi} = 5.37 \times 10^{3} \quad \frac{\text{meter-sec}}{\text{kgm}}$$

$$\sigma = 10^{4} \quad \frac{\text{mhos}}{\text{meter}}$$

$$(P_r)_a = 10^{10} \quad \frac{\text{watts}}{\text{meter}^3}$$

$$\frac{h_1}{RT_o} = 1000$$

An estimate can now be made for the magnitude of the error introduced by assuming that the discharge extended to the wall. The outer solution can be written as:

$$\frac{h_1 - h_w}{r_1 q_w} = \frac{\frac{dh}{d\phi}\frac{R}{r_1}\ln\frac{R}{r_1}}{\frac{\frac{1}{2} + \frac{3}{2}(R_e)_M + \frac{5}{6}(R_e)_M^2}{\left[1 + (R_e)_M\right]^2}} \qquad (29)$$

Since the expression containing $(R_e)_M$ varies for 1/2 to 5/6 as $(R_e)_M$ goes from 0 to infinity, a value of 0.65 is assigned to it. For arc radii varying from 10 cm to 1 cm then the radius ratio varies from 1.01 to 1.10. This indicates that there is only a small error, at most 10%, introduced into the calculation, by assuming that the arc fills the constrictor.

As in the previous case, values can be assigned to the parameter $(R_e)_M$, and relations found among the average gas pressure $\frac{p_{av}}{p_a}$, the radially-averaged gas enthalpy $\frac{h_{av}}{RT_o}$, the arc current I, the constrictor radius R and the power in the gas, P_{c}^{o}. Data from this evaluation have then been plotted on Figs. 16, 17, and 18, the maps of h/RT_o vs p/p_o for air arc heaters for values of h/RT_o greater than 1000.

Viewing Figs. 16, 17 and 18 as a whole, there is a general sweep from the low pressure, high enthalpy, high current, large size regime out to the high pressure, lower enthalpy, low current small size regime. The power in the gas is a weak function of both pressure and enthalpy in the low enthalpy regime, but climbs steeply in the high enthalpy regime, indicating that a great deal of power is going to be needed to realize the higher-than-state-of-the-art enthalpies that the calculations indicate are feasible.

5. CONCLUSIONS AND SUGGESTED FUTURE WORK

For the design optimization of high enthalpy arc heaters the Stine-Watson type of analysis, when extended to include radiation, gives adequate semi-empirical formulas for all the gases investigated. That is, the dimensionless parameters derived from this model adequately represent the dominant physical effects, and the constants can be empirically adjusted to absorb the major errors introduced by the simple model.

To obtain a more accurate theoretical description of the inlet regime, one may have to simultaneously include the effects of the axially varying discharge cross section, pressure and velocity distributions including the contributions due to magnetic pumping, and of course, the nonlinear material functions*. The mathematical complexity of this problem then would be of a totally different order, namely that of a complete, nonlinear, two-dimensional magnetogasdynamic-viscous flow problem. To the writer's knowledge, there exists no general mathematical approach, numerical or other, capable of solving this very complicated and very nonlinear problem with any "reasonable" expenditure of computing hours. It is thus clear that one will have to rely upon highly simplified analytical models for some time to come.

For the necessarily rough estimates of the ultimate performance limits, i.e., for the hot gas containment limit calculation, the asymptotic column results appear adequate. This is understood when we consider, first, that the fully developed column solution is the condition which the gas flow at the heater outlet must approach asymptotically, and second, that in the region where the flow does approach the fully developed solution the wall heat load is roughly proportional to the average gas enthalpy at each cross section, as shown by the extended Stine-Watson analysis and by experiment.

The important result of this containment limit calculation is the theoretical prediction of an optimum constrictor size for all cases for which the "optically thin gas" approximation reasonably

*However, the possibility exists that the radius-of-arc to radius-of-wall ratio, r_1/R, may be advantageously introduced into the Stine-Watson theory by itself.

well represents the total radiation from the arc. This optimum constrictor radius varies with pressure like the square root of the radiation intensity P_r. That is, $R_{opt} \sim \propto (P/P_o)^{1/2}$ at the lower enthalpies and $R_{opt} \sim \propto (P/P_o)$ at the highest enthalpies. The existence of this optimum radius implies an "absolute" containment limit as long as we remain in the thin gas regime. Only for very much larger sizes, i.e., when the constrictor radius becomes much larger than the optical path length L.*, will this qualitative trend reverse itself, as shown in the following sketch:

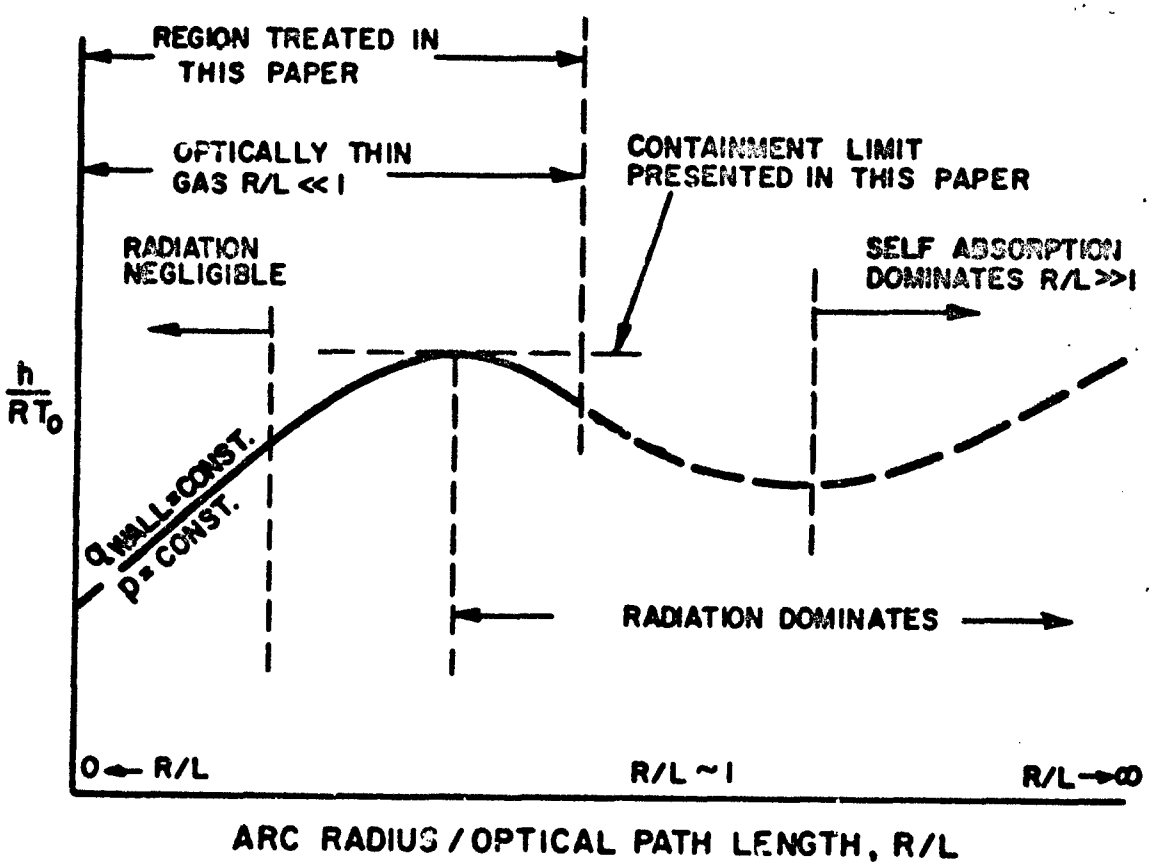

* The optical path length L is defined as $1/\alpha$, i.e., the inverse of the absorption coefficient per unit length, α. Thus in a gas of constant conditions the radiation from a point is attenuated by a factor $e^{-\alpha L} = e^{-1}$, in a distance L.

For many arc applications with gases like hydrogen or nitrogen the optically thin gas regime treated here covers the sizes and pressures of practical importance. However, for other gases such as mercury and alkali metal vapors, as well as for extremely high pressures with nitrogen, the "optically dense" gas regime is of practical importance. This should be treated in a future calculation.

It should be pointed out that, for the asymptotic or fully developed column theory, there are no fundamental mathematical obstacles which would prevent us from making the calculation more accurate. The problem is one-dimensional and the energy equation is virtually decoupled from the momentum and continuity equations except for the magnetically induced radial pressure gradient. Thus the inclusion of the exact material functions, of self absorption and magnetic pressure simply make the energy equation more complicated and more non-linear, but do not prevent the use of numerical successive approximation (Piccard type) solutions which can be made "as accurate as we please," certainly as accurate as our knowledge of the material function curves would warrant. This is contrasted with the at least two dimensional* inlet problem where the coupling between momentum and energy equations is strong and essential. Thus the fully developed column solutions with radiation and magnetic pressure, and the integrated enthalpy of the flowing gas for this case, can, and undoubtedly will, be calculated much more accurately than was done here.

A final important open question, and a possible error in this and most other analyses of the coaxial flow discharge, is the apriori assumption of laminar flow. It is quite possible, even probable, that turbulence-like disturbances may be created in the discharge itself. From the "kink" instability of the arc one would expect this tendency. However, besides our present inability to calculate a "turbulent" flow discharge, there are justifications for working with a purely laminar flow model in practice. They are:

1. That the mean Reynolds numbers are in most cases extremely low, due to the high viscosities of the ionized gas,

---

* Some instabilities (secondary flow) could here even destroy the axial symmetry and make the flow problem three dimensional. Such cases are believed to have been observed.

so that the damping of disturbances must be very high.

2. That the flow near the walls, where the thermal impedance is highest, is believed to be stabilized by the temperature and viscosity gradient there ("Lees' effect"), and
3. That for the few cases for which complete comparisons have been carried out, namely for nitrogen arcs (Ref. 26) excellent agreement between theoretical and experimental thermal conductivities was obtained with the laminar model.

The comparison between the gas heater state of the art performance envelope and the theoretical containment limit curves, rough and tentative as it undoubtedly is, still leads to the conclusion that there appears to be considerable "room" for substantial advances in gas heater performance, i.e. for higher mean enthalpies at all pressure levels, but most of all at the lower pressures. We note first that a well cooled thin metal wall can stand heat loads of 10-15 kw/cm^2 (plane slab conduction and cooling) and even higher values when we deal with a very small or very short cylindrical channel (three dimensional conduction). However, in gas heater practice where there may be neither free choice of the metal nor of the geometry, 1-3 kw/cm^2 appear reasonable wall heat load values for high pressure water cooled parts.

Now we compare on the pressure-enthalpy charts, Figs. 16 through 18, the empirical arc air heater performance envelope with the containment limit curves for 1 kw/cm^2 and for 3 kw/cm^2. Even the lower one of these lies appreciably above the "state of the art" envelope. If we assume the containment limit curves to be sufficiently accurate for this type of comparison (i.e. say reliable within a factor of 2) then we must ask why gas heaters have not yet gotten up into the regime between the two containment curves mentioned. Part of this might be attributed to deviations from what is now believed to be the optimum size for containment, or to insufficient constrictor heat load capability (e.g. ceramic-lined constrictors). However, these

explanations are not sufficient to bridge the gap.

The major reason must be that physical mechanisms other than the simple hot gas containment have limited the performance of the arc gas heaters built to date. In most arc heater designs the electrodes are exposed to the full containment heat loads plus large additional heat loads at the arc attachment points, so that the electrodes clearly are the performance limiting components. This is especially true at the low pressures where the total current values required to reach the containment limits become very large.

However, we know that there are possible methods and design configurations which remove the electrodes from becoming the performance limiting components. The "Double Gerdien" arc chamber (Ref. 27 and 28) is one of these configurations, and there are others. It is this reasoning which led us to calculate the containment limit as the most likely performance boundary. Therefore, we conclude that arc gas heater performance corresponding to the appropriate containment limit curves (perhaps the 3 kw/cm^2 curve) should be technically possible.

For more accurate predictions it will be necessary to recalculate these curves more precisely for the optically thin gas, to calculate the "optically dense" gas regime also, and, most important, to check these theoretical predictions with suitable experiments.

REFERENCES

1. G.L. Cann, "Energy Transfer Processes in Partially Ionized Gases," Ph.D. Thesis, California Institute of Technology, (June 1961). (Also published as GALCIT Hypersonic Research Project Memorandum No. 61)

2. R.D. Buhler, "Electrothermal Propulsion", Chapter in "Advances in Space Propulsion" (Simkin-Szego, Ed.) John Wiley and Sons, (to be published in 1964)

3. J. Uhlenbusch, "Zur Theorie und Berechnung Stationarer und Quasistationarer Zylindrischer Lichtbogen," Doctoral Dissertation, Technical University, Aachen, 1962

4. H. Maecker, "Uber die Charakteristiken Zylindrischer Bogen," Zeit f. Phys., 157, 1-29 (1959)

5. M. Chen, "Theory for a Fully-Developed, Laminar, Axial Positive Column," AVCO RAD Internal Memo 8-10-61; also: Paper Presented at Symposium for Engineering Aspects of Magnetohydrodynamics, Berkeley, Calif., April 1963

6. G. Kirschstein and F. Koppelmann, "Der Elektrische Lichtbogen in Schnellstroemendem Gas", Wiss. Veroeff. a.d. Siemens Werken, Vol. XVI Heft 1 (Part 1) and Vol. XVI Heft 3 (Part II), March and August 1937, Also: Koppelmann: Z. Techn. Physik 15, p. 604, (1934)

7. A.M. Cassie, "Some Theoretical Aspects of Arcs in Nozzles under Forced Convection," Proceedings of the Fifth International Conference on Ionization Phenomena in Gases, Munich, 1961, North Holland Publishing Co., Amsterdam

8. H.A. Stine and V.R. Watson, "The Theoretical Enthalpy Distribution of Air in Steady Flow Along the Axis of a Direct-Current Electric Arc," NASA TN D-1331 (August 1962)

9. J. Skifstad and P. Murthey, "Analysis of Arc Heating Phenomena in a Tube," Presented at International Symposium on Plasma Phenomena and Measurements, San Diego, November 1, 1963

10. R.R. John, M. Chen, et al, "Theoretical and Experimental Investigation of Arc Plasma-Generation Technology", Technical Documentary Report ASD-TDR-62-729, Part II, Vol. 2, Section III (September 1963)

11. G.L. Cann, R.D. Buhler, J.M. Teem, L.K. Branson, "Magnetogasdynamic Accelerator Techniques," Rpt. No. AEDC-TDR-62-145, July 1962

12. J. M. Yos, "Transport Properties of Nitrogen, Hydrogen, Oxygen and Air to 30,000 $^{\circ}$K", AVCO Tech. Memo RAD-TM-63-7, Contr. AF33(616)-7578, Task 73603, 22 March 1963

13. E. Baum, G. L. Marlotte, "Calculations of Transport Properties and Specific Radiated Power for Argon Gas," Unpublished

14. G. Schmitz, H. J. Patt and J. Uhlenbusch, "Eigenschaften und Parameterabhangigkeit der Temperaturverteilung und der Charakteristik eines Zylindersymmetrischen Stickstoffbogens", Zeitschrift fur Physik 173, 552-567 (1963)

15. T. Peters, "Bogenmodelle und Steenbeckscher Minimumprinzip," Proceedings Fifth International Conference on Ion Phenomena in Gases, Munich (1961), North Holland Publishing Co., (1962)

16. J. G. Skifstad, "Investigation of a DC Arc Stabilized in a Cylindrical Tube," Final Report Contract nonr 1100 (17), Jet Propulsion Center, Purdue University, (1962)

17. H. Maecker, Messung and Auswertung von Bogencharakteristiken (Ar, N_2), Z. fur Phys. 158, 392-404 (1960)

18. H. Brinkmann, "Optical Studies of the Electric Arc Light" (in Dutch), Dissertation. Utrecht - Amsterdam (1937); also L. S. Onstein and H. Brinkmann, Proc. Amst. 34, 498 (1930) and Physica, Haag, 1, 797 (1934) and D. Th. J. Ter Horst, Dissertation, Utrecht (1934)

19. O. Koch, K. J. Lecermann and A. Walther, Z. Physik 127, 153 (1950)

20. L. A. King, Theoretical Calculation of Arc Temperatures in Gases, Colloquium Spectroscopicum International VI (Amsterdam, 1956), p 152 (London-Pergamon Press 1957) (Based on E.R.A. Report, Ref. G/XT155)

21. G. L. Marlotte, "Numerical Integrations of Arc Column Energy Balance Including Radiation" (to be published)

22. Cann, G. L., et al "Thermal Arc Jet Research" (U), Aeronautical Systems Division, Technical Documentary Report No. ASD-TDR-63-632, Contract No. AF33(657)-8839, Electro-Optical Systems, Inc., (15 August 1963) Confidential

23. H. W. Emmons and R. I. Land, "Poiseuille Plasma Experiment", The Physics of Fluids, Vol. 5, No. 12, December 1962

24. C. E. Shepard and V.R. Watson, "Performance of a Constricted-Arc Discharge in a Supersonic Nozzle", AIAA Preprint 63-380 (Presented at Biennial Gas Dynamics Symposium, Northwestern University, August 1963)

25. Kotanchik, J. N. and Greenshields, D. H., Facilities for High-Temperature Flight Environment Simulation, Aerospace Engineering 22, No. 1, 1963.

26. Schmitz, G., and Patt, H. J., "Die Bestimmung von Materialfunktionen eines Stickstoffplasmas bei Atmospharendruck bis 15000°K," Zeit. f. Physik, 171, 449-462 (1963).

27. Weber, H. E. and McGinn, J. H., A Constricted Arc for High Energy Gas Flow, Aerospace Engineer 22, No. 1, 1963.

28. Pugmire, T. K. Weber, H. E. and Marston, C. H., "Arc Heater Development for Entry Simulation," G. E. Space Sciences Laboratory Report #R63SD49 (October 1963).